Computer Networks 251 (2024) 110627

Contents lists available at ScienceDirect

Computer Networks

journal homepage: www.elsevier.com/locate/comnet

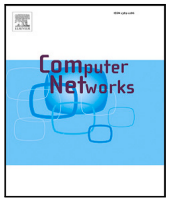

Multi-objective optimization of asymmetric bit rate partitioning for multipath protection in elastic optical networks

Henrique A. Dinarte [c,*], Karcius D.R. Assis [b], Daniel A.R. Chaves [c], Raul C. Almeida Jr. [a,d], Raouf Boutaba [d]

[a] Eletronics and Systems Department, Federal University of Pernambuco, Recife, PE, Brazil
[b] Electrical and Computer Engineering Department, Federal University of Bahia, Salvador, BA, Brazil
[c] Polytechnic School of Pernambuco, University of Pernambuco, Recife, PE, Brazil
[d] David R. Cheriton School of Computer Science, University of Waterloo, Waterloo, ON, Canada

ARTICLE INFO

Keywords:
Elastic optical networks
RMSA
Multipath provisioning
Multipath routing
Squeezed bandwidth protection
Network survivability
Multi-objective optimization
Genetic algorithm

ABSTRACT

In survivable elastic optical networks, multi-path protection combined with traffic squeezing has gained attention. Link-disjoint multipath routing (LD-MPR) and bandwidth squeezing protection (BSP) when applied to the routing, modulation level and spectrum assignment problem are efficient strategies to address the excessive bandwidth demanded by protected services, spectral fragmentation and link-load balancing. LD-MPR enables the division of service transmission bit rate into independent flows, whereas BSP tolerates traffic reduction under link failure. An open issue in the literature is how to efficiently divide demanded traffic among the link-disjoint routes under dynamic-traffic and BSP, while complying the service level agreement (SLA). We propose in this paper a multi-objective-optimization genetic algorithm that defines how service transmission bit rate should be partitioned among the candidate link-disjoint routes. A customized partitioning definition is made for each source–destination node pair in the network, aiming the simultaneous minimization of network blocking probability and average squeezing transmission bit rate experienced by the services during single-link failure. We also propose, a fixed-alternate routing using groups of disjoint paths (FARgdp). Complex dynamic-traffic network scenarios that simultaneously consider BSP, LD-MPR and FARgdp are addressed.

1. Introduction

A classical problem in elastic optical networks (EON) is the routing, modulation level and spectrum assignment (RMSA) problem [1–4]. It consists of finding a route, a modulation format and a suitable spectral band to properly allocate the transmission bit rate demanded by a network service [1,2]. There are two constraints that must be observed by an RMSA solution throughout the chosen route: (a) the use of adjacent slots in frequency, as well as, (b) the use of the same spectral range along the route links [1,2]. These two constraints are known, respectively, as spectral contiguity constraint (SCgC) and spectral continuity constraint (SCnC) [1,2]. The observance of both SCgC and SCnC on allocating successive heterogeneous services (i.e. services that require different transmission bit rates) on the network may generate a misalignment between the available frequency slots in network links, a situation known in the literature as spectral fragmentation (SF) [1,2,5,6]. A spectrally fragmented network may have several available slots in its links, but not adjacent to each other, which may prevent the establishment of a large number of services due to SCgC and SCnC enforcement. A way to mitigate the deleterious effect of SF is to apply multipath provisioning (MPP) [5,7–9]. In it, the SCgC is partially relaxed, as the total transmission bit rate required by a service can be divided into several independent flows, each of which may be transmitted over the network using different routes with individually contiguous spectral bands [5,8,9]. A possible drawback of using MPP is the use of a separate spectral guard band (GB) for each flow, instead of using a unique GB when single-path provisioning is adopted [9]. The multipath strategy in EONs is mainly enabled by the use of sliceable bandwidth variable transponders (SBVT) [1,10]. The acronyms mentioned in our paper are listed in Table 1. In the MPP strategy, multiple P routes (say the routes $r_1, \ldots, r_P$) are chosen to transmit the P flows generated by the division of the original transmission bit rate of the service. These routes may, or may not, be link-disjoint [9,11]. We name the first case (assuming link-disjoint routes) as link-disjoint multipath

* Corresponding author at: Polytechnic School of Pernambuco, University of Pernambuco, Recife, PE, Brazil.
E-mail addresses: henrique.dinarte@upe.br (H.A. Dinarte), karcius.assis@ufba.br (K.D.R. Assis), darc@ecomp.poli.br (D.A.R. Chaves), raul.almeidajunior@ufpe.br (R.C. Almeida Jr.), rboutaba@uwaterloo.ca (R. Boutaba).

https://doi.org/10.1016/j.comnet.2024.110627
Received 7 February 2024; Received in revised form 10 May 2024; Accepted 1 July 2024
Available online 8 July 2024
1389-1286/© 2024 Elsevier B.V. All rights are reserved, including those for text and data mining, AI training, and similar technologies.

Table 1
List of acronyms.

Acronym	Definition
BP	Blocking Probability
BSP	Bandwidth Squeezing Protection
DPP	Dedicated Path Protection
DPPS	Dedicated Path Protection with Squeezing
DPGR	Disjoint Path Group Routing
DPGR-Multi-P	Disjoint Path Group Routing with Multiple Paths
EON	Elastic Optical Network
FARgdp	Fixed-Alternate Routing using groups of link-disjoint paths
GB	Guard Band
LD-MPR	Link-Disjoint Multipath Routing
MPP	Multipath Provisioning
NSGA-II	Non-dominated Sorting Genetic Algorithm II
OPDPP	Optimized Partitioning Dedicated Path Protection
OSNR	Optical Signal-to-Noise Ratio
P	Number of link-disjoint paths
PDPP3	Partitioning Dedicated Path Protection with 3 paths
$PDPP3S_F$	Partitioning Dedicated Path Protection with 3 paths, Squeezing and FARgdp
RMSA	Routing, Modulation Level, and Spectrum Assignment
RSA	Routing and Spectrum Assignment
SBVT	Sliceable Bandwidth Variable Transponder
SCgC	Spectrum Continuity Constraint
SCnC	Spectrum Contiguity Constraint
SF	Spectral Fragmentation
SLA	Service Level Agreement
SPP	Single Path Provisioning
TRaP	Transmission-Bit-Rate Asymmetric Partitioning
TRsP	Transmission-Bit-Rate Symmetric Partitioning

routing (LD-MPR), and it has direct application to provide link failure resilience to the network [8,12–14].

Solving the RMSA problem and yet providing network survivability is an important issue in optical transport networks [15–18]. Protection is one of the survivability mechanisms most used in optical networks, since it provides faster traffic recovery when compared to other survivability methods, for instance restoration [8,14,15,19]. Whereas the restoration strategy searches for alternative routes upon a failure occurrence, the protection scheme, on the other hand, reserves (prior to failure occurrence) enough extra resources for guaranteeing the service of each connection under failure occurrence.

In EONs under dynamic traffic, two types of provisioning are usually used by the protection schemes: the classical single-path provisioning (SPP) and the previously defined LD-MPR [11,12]. In SPP, two link-disjoint lightpaths, referred to as working and backup lightpaths, are both established with enough capacity to transmit the requested bit rate [15]. In this case, the required bit rate is twice the requested one and, whenever a failure occurs in the working lightpath, its traffic is entirely switched to the backup ligthpath. Differently from SPP, in LD-MPR there is no exclusive lightpath operating as either working or backup [12,13]. Instead, LD-MPR proposes the partitioning of the total transmission bit rate into multiple portions of lower rates, which are transmitted simultaneously through multiple disjoint lightpaths. In LD-MPR, the total transmission bit rate (B_t) required to provide protection for a service is evaluated from the service's requested transmission bit rate (B_r). Then, B_t is divided into P disjoint routes so that, if there is a failure in one of the P disjoint routes, the remaining $P-1$ routes are capable of transmitting at least the transmission bit rate B_r.

Another important survivability strategy in EONs is Bandwidth Squeezing, in which the requested transmission bit rate may be reduced to at most a certain squeezing factor (β) under a failure in one of the links used by the service. Under Bandwidth Squeezing Protection (BSP), the transmission bit rate of the service is reduced to at most $(1-\beta)B_r$ under failure event. A proper value of β is crucial, which shall be agreed between the network operator and the service customer via service level agreement (SLA). BSP is an attractive strategy to operators because it provides a positive trade-off between revenue and network availability [19].

The total transmission bit rate using LD-MPR approach is influenced by two factors: the allowance (or not) of bandwidth squeezing under a failure and how the transmission bit rate is distributed among the link-disjoint routes [20]. The total transmission bit rate required by the service may be equally divided among the P disjoint lightpaths of the service (Assis et al. [12,13]) or unequally divided (Takeda et al. [11,21]). The former strategy is named in this paper as transmission-bit-rate symmetric partitioning (TRsP) whereas the latter is named as transmission-bit-rate asymmetric partitioning (TRaP).

One of the most used strategies to solve the routing problem in optical networks is fixed-alternate routing (FAR) [1]. In FAR, an ordered set O, composed of K candidate routes ($O = \{r_1, \ldots, r_K\}$), is calculated between each source (i) and destination (j) pair of network's nodes [1]. For example, the set O can be composed of the K shortest paths between s and d, sorted in ascending order. To establish a service request S between the $i-j$ nodes, the routes in O are successively tested (from the first to the Kth route) until a route with sufficient spectral availability to fit the allocation of S's transmission bit rate is found [1]. FAR is known in the literature for making a good compromise between computational complexity and network performance [1]. FAR optimizes resource utilization by dynamically redistributing traffic across multiple paths, thereby increasing the network's ability to support a larger volume of traffic loads. No efficient FAR strategy has been proposed in the literature to solve routing in EONs considering either multipath or LD-MPR scenarios. Nevertheless, FAR strategy can also be adapted to enable the establishment of protected services that utilize LD-MPR. We name this strategy in this paper as fixed-alternate routing using groups of disjoint-paths (FARgdp). In FARgdp strategy, the original set of candidate routes is transformed into a set of groups of candidate routes, each group containing P disjoint routes. The set of candidate groups of disjoint-paths between $i-j$ is now defined as $O = \{g_1, \ldots, g_K\}$ in which $g_k = \{r_{1,k}, \ldots, r_{P,k}\}$, providing that the routes $r_{i,k}$ and $r_{j,k}$ are link-disjoint for $i \neq j$ and $k \in \{1, \ldots, K\}$. To the best of our knowledge, this paper introduces the FARgdp concept, with a detailed description and application of it in optical networks, and proposes a suitable algorithm to implement this concept in practice.

Consider the link-disjoint routes $(r_{1,k}, \ldots, r_{P,k})$ in a group g_k that belongs to the set of candidate groups evaluated for a given source–destination ($i-j$) node pair under the FARgdp strategy. Such routes may have different topological (e.g. hop counting or physical length) and operational (more or less traffic congestion) characteristics. Therefore,

an unequal partitioning of B_t among these routes, by applying the TRaP strategy, may enable a more efficient transmission bit rate division if compared against the TRsP strategy. For instance, on using the TRaP, higher amounts of transmission bit rate may be allocated on the shorter routes of the group, enabling that a great part of the transmission bit rate be transmitted using a more spectrally efficient modulation format and, as a consequence, using less network spectrum [11]. On the other hand, under the same scenarios, the B_t required by the TRaP strategy is always greater than that required using TRsP. Then, a careful asymmetric assignment must be chosen in order to bring benefits towards a better spectral occupation of the network. Other benefits from the use of TRaP are further discussed in the article.

Clearly, considering an elastic optical network under dynamic traffic, it is not an easy task to find a suitable form of partitioning the B_t of a service in a network scenario that simultaneously considers TRaP, FARgdp and BSP strategies. This choice impacts the network spectrum occupation, and, therefore, the network performance in terms of blocking probability, as well as the average squeezed transmission bit rate suffered by a service in the event of a link failure. Under TRaP, the squeezed transmission bit rate actually experienced by a service S depends, specifically, on which of the P routes serving S has failed, which is not the case under TRsP. It is possible to evaluate the average squeezed transmission bit rate (in the event of a failure) suffered by all established services in the network by the manner on how B_t is partitioned for each service and the failure probability of the P routes used by each service. Note that, from the network operator point of view, such average squeezed bit rate to which the services are submitted and the network blocking probability (BP) are conflicting optimization goals. Allowing an increase in the average squeezed bit rate experienced by a service during its link failures demands from the network lower bandwidth portions. This reduction in required bandwidth leads to a more efficient utilization of network resources (fiber spectrum), resulting in a reduction in overall network blocking probability. By reducing the utilization of available bandwidth as a consequence of increasing average squeezed bit rate, the network can better accommodate its traffic demands and, therefore, minimize the likelihood of traffic blocking. The opposite reasoning is also true. Therefore, one idea developed in this paper is to propose/analyze forms of reducing the average squeezing factor but committed to keep/reduce the network blocking probability. Notice that this is a multi-objective optimization problem of great interest to network operators since its solution allows finding the best trade-off between network performance (in terms of BP) and network resilience to failures (in terms of average squeezed bit rate). Moreover, this is also a nonlinear multi-objective optimization problem, which prevents the use of efficient classical optimization algorithms to solve it [22]. Therefore, it is necessary to employ heuristics or metaheuristics to find optimized solutions [23]. Several metaheuristics have been successfully applied to perform optimization in different optical networking problems, reaching near-optimal solutions in several cases [2,4,16,17,24–35]

1.1. Objective and contribution

In short, in this paper we propose a multi-objective optimization genetic algorithm that defines how the services' transmission bit rate should be partitioned among the candidate link-disjoint paths. A customized partitioning definition is made for each pair of $i-j$ nodes in the network, and the aim of the proposed optimization procedure is to simultaneously minimize the network blocking probability and the average squeezed bit rate experienced by the services in the network during a link failure. Particularly, in this paper we are considering the complex network scenario under dynamic traffic which simultaneously considers bandwidth squeezing protection (BSP), link-disjoint multipath routing (LD-MPR) and asymmetric bit rate partitioning (TRaP). Under this scenario, to the best of our knowledge, the contributions of this paper are:

- Application of a multi-objective Evolutionary Optimization Algorithm to address a real world complex problem faced by multipath routed optical networks on providing survivability against network hardware failures (fiber optics) under a dynamic (stochastic) traffic pattern;
- Specifically, we utilize the multi-objective optimization genetic algorithm (NSGA-II) to efficiently determine a set of solutions for transmission bit rate partitioning on a per node-pair basis among the candidate multipaths. This approach enables us to achieve an optimized trade-off between network performance and resilience. To the best of our knowledge, this paper is the first in the literature to explicitly address and investigate this trade-off.
- The proposal and application of the fixed-alternate routing procedure that uses groups of link-disjoint paths (FARgdp), together with an algorithm to create the groups of link-disjoint paths;
- The application of Asymmetric Bit Rate Partitioning in a dynamic-traffic scenario, as well as, finding optimized solutions for asymmetric transmission bit rate partitioning among the routes which compete for the network resources. To the best of our knowledge, this paper is the first in the literature to address the application of Asymmetric Bit Rate Partitioning in a network under dynamic-traffic;
- The introduction of a new metric for resilience evaluation: the average squeezed transmission bit rate experienced by the services during a link failure;

1.2. Structure of the paper

The paper is organized as follows. Section 2 presents some relevant related works and the its mainly differences to our proposal. Section 3 describes the symmetric and asymmetric transmission-bit-rate partitioning. Section 4 details the optimization problem formulation. Section 5 shows an overview of algorithms and strategies proposed in this paper. Section 6 presents a proposed fixed-alternate routing by groups of disjoint paths. Section 7 details our proposed meta-heuristic. Sections 8 and 9 present, respectively, the simulation setup and the discussion of the results with some highlights. The conclusion is given at the end of the paper (Section 10).

2. Related works

Two main difficulties in providing resilient services in EONs are the spectral fragmentation and the excessive allocation of bandwidth necessary to provide such resilience. The joint application of LD-MPR and BSP techniques works towards mitigating these two difficulties, as they enable several optimization opportunities and, consequently, improvements on network performance. For this reason, protection schemes based on either LD-MPR or BSP have recently aroused great interest among researchers [5,6,11,17,18,36]. The multipath protection problem has been extensively studied in the literature, considering solely the TRsP strategy in static traffic scenarios [11,17,37–39]. However, the application of TRaP in networks with dynamic traffic remains almost unexplored.

Paira et al. [6] present a novel fragmentation-aware and energy-efficient multipath-based protection scheme named P-EM-RSA for prioritized connections in dynamic EON. Their heuristic focus on minimizing total network power consumption, by reducing the usage of various network elements and network spectrum occupation, so that the bandwidth blocking ratio may be reduced without compromising any high priority connections. The work also applies the BSP strategy.

Assis et al. [12,13] investigated dedicated path protection (DPP) scheme and proposed a traffic partitioning scheme, referred to as Partitioning Dedicated Path Protection (PDPP). DPP is a SPP-based scheme that protects the requested traffic by setting up working and backup lightpath with identical capacities. This incurs in doubling the required network capacity. On the other hand, PDPP does not employ

the isolated concept of working and backup lightpaths, but performs traffic partitioning among multiple link-disjoint lightpaths. The authors show that PDPP is capable of saving substantial network resources when compared to DPP. PDPP uses a symmetrical traffic partitioning (i.e. applies TRsP) among the link-disjoint paths and can also employ BSP for further network resource savings.

Takeda et al. [11,21] applies a LD-MPR-based protection scheme and introduce the TRaP strategy. ILP models are presented to find the optimal asymmetrical transmission bit rate distribution among the routes. The ILP is applied either considering a given set of pre-computed link-disjoint routes (FSA-NPS) or computing link-disjoint routes alongside with the asymmetric transmission bit rate distribution (RFSA-NPS). The described ILP methods are capable to find the optimum solution only for a single incoming service in the network. Clearly, it is not a practical network scenario in which several services are simultaneously allocated in it (*i.e.* dynamic traffic). Assis et al. [3] also investigate the application of ILP models assuming TRaP, but considering static traffic and no spectral assignment.

The works by Halder et al. [16,17,22] investigated the provisioning of protected services under the LD-MPR scenario and also utilized genetic algorithm to find optimized solution for paths and regeneration sites selection [17], routing paths and fiber core selection [22] and decision on how many division (either 2 or 3) the service is segmented [16]. All works consider a static traffic scenario.

Let us now discuss some conceptual differences among our work and the previously mentioned articles. In terms of the application of the TRaP strategy, differently from [11,21], we propose an optimized asymmetric partitioning of services' transmission bit rate among the link-disjoint paths considering a network scenario in which there are several services competing for the network resources. Moreover, our proposal also takes into account loading balancing issues among the services that is not taken into account in [11,21]. Differently from [3], we are considering dynamic traffic and spectral assignment. In terms of the application of the genetic algorithm strategy, our proposed genetic-algorithm optimization is focused on how to optimize the division of services' transmission bit rates among the link-disjoint routes, whereas the works [16,17,22] are focused on finding the routes itself. Notice that we also mention in the last paragraph of Section 1 some contributions that, to the best of our knowledge, do not present counterparts available in the literature.

3. Symetric vs. asymmetric transmission-bit-rate partitioning in link-disjoint multipath routing

To properly discuss the particularities about the application of TRsP and TRaP strategies under LD-MPR regime, we give examples of both strategies in Sections 3.1 and 3.2. In Section 3.1, the DPP and PDPP strategies [13] are used as a starting point for such comparison. The latter is a SPP strategy and the former a LD-MPR strategy. In the discussions, a numeric suffix is appended to the strategy's name to indicate the number of used link-disjoint paths, and the "S" suffix is appended to indicate the application of the BSP premise (e.g. PDPP3S considers 3 link-disjoint paths and BSP, whereas PDPP2 considers 2 link-disjoint paths and do not allow BSP). In Section 3.2, the strategies are adapted to employ TRaP.

3.1. Transmission-Bit-Rate Symmetric Partitioning (TRsP)

Fig. 1 shows an example of a 100 Gb/s connection between the node pair 0–2, established using DPP (Fig. 1a and c) and PDPP3 (Fig. 1b and d) schemes. The solid line in blue color represents the working path, while the dashed line represents the protection path. DPP (Fig. 1(a)) allocates $B_r = 100$ Gb/s on the working path and additional 100 Gb/s on the protection path, resulting in $B_t = 200$ Gb/s. On the other hand, PDPP3 (Fig. 1(b)) splits B_t equally into 3 partitions of 50 Gb/s and transmits them over three disjoint paths, leading to $B_t = 150$ Gb/s. Note that in both cases the same level of resilience against a single link failure is achieved, but the use of PDPP scheme leads to a 25% reduction in B_t allocated when compared to DPP. These partial transmission bit rates are referred to as split bandwidth (B_s):

$$B_s = \frac{B_r}{P-1}, \tag{1}$$

where P is the number of disjoint paths used by the protection scheme (in this paper we assume either $P = 2$ or $P = 3$ for the PDPP). In case of a single-link failure, full traffic protection is guaranteed, since the aggregated bit rate of the remaining $P-1$ routes is B_r. During normal operation, B_r out of B_t is the effective required bit rate, which allows the incremental bandwidth $B_i = B_t - B_r$ be used for additional data transmission or connection robustness enhancement with the use of a more efficient forwarding error correction (FEC) encoding. This advantage is not possible in DPP, since its working and protection traffics are not combined but only switched at the end nodes.

To assess the use of LD-MPR with BSP, Assis et al. [13] introduced two parameters: bandwidth squeezing factor (β) and bandwidth-increment factor (α). The bandwidth squeezing factor corresponds to the maximum service's transmission bit rate percentage reduction under a single-link failure. This factor is usually set in the service level agreement (SLA) and defines the maximum amount of transmission bit rate that can be suppressed during a failure ($B_{sq} = \beta B_r$) or, analogously, the portion of traffic, B_x, that remains active during a failure, where $B_x = B_r - B_{sq} = (1-\beta)B_r$. By allowing BSP, the β parameter is taken into account and the evaluation of B_s is updated to:

$$B_s = \begin{cases} \dfrac{(1-\beta)\cdot B_r}{P-1}, & if \quad \beta \le \dfrac{1}{P} \\ \dfrac{B_r}{P}, & otherwise. \end{cases} \tag{2}$$

The value of β is related to B_{sq}, B_r and B_x by

$$\beta = \frac{B_{sq}}{B_r} = \frac{B_r - B_x}{B_r}. \tag{3}$$

Note from Eq. (3) that β value is inside the $0 \le \beta \le 1$ interval. The lower is the value of β the lesser is the service suppressed transmission bit rate during a failure event. In particular, $\beta = 0$ means $B_r = B_x$, which corresponds to the scenario where no squeezing is applied during a failure. From Eq. (2), one may notice that $\beta = 1/P$ is automatically achieved if no extra transmission bit rate is allocated (i.e. by setting $B_t = B_r$). Therefore, β values in range $1/P < \beta \le 1$ is not object of interest.

The bandwidth increment factor is related to the necessary additional transmission bit rate (B_i) allocated to ensure the desired protection/squeezing level. The specific value of the α parameter is a consequence of the choice made for the value of β, and it can be calculated by

$$\alpha = \frac{B_i}{B_r} = \frac{B_t - B_r}{B_r}. \tag{4}$$

Figs. 1(c) and 1(d) show an example of a connection establishment using DPPS and PDPP3S schemes, respectively, assuming in both cases the maximum squeezing of 20% ($\beta = 0.2$). DPPS establishes a single protection path considering such a reduction, which leads to $B_t = 180$ Gb/s and $\alpha = 0.8$. On the other hand, for the same squeezing factor of $\beta = 0.2$, PDPP3S partitions the traffic among three paths and applies the BSP to operate with $B_s = 40$ Gb/s on each link-disjoint path, leading to $B_t = 120$ Gb/s and $\alpha = 0.2$ (Fig. 1(d)). Note that, in both referred policies that allow squeezing, $B_x = 80$ Gb/s is guaranteed under single-link failure. In addition, policies that apply traffic partitioning, as in PDPP and PDPPS, use less resource than DPP and DPPS, respectively.

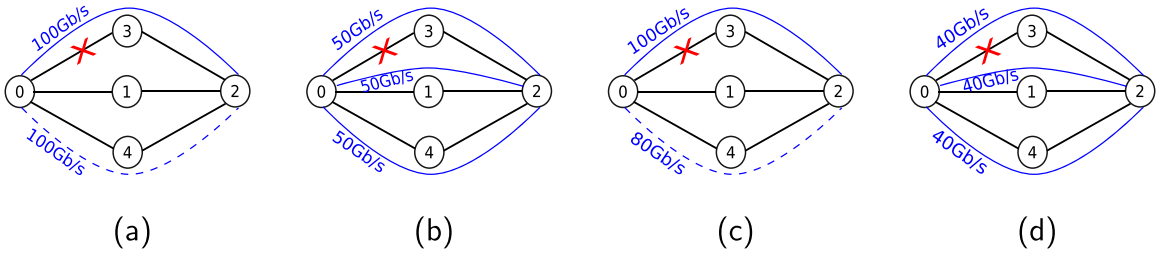

Fig. 1. Example of connection between nodes 0 and 2 (B_r = 100 Gb/s) established by: (a) DPP (β = 0), (b) PDPP3 (β = 0), (c) DPPS (β = 0.2) and (d) PDPP3S (β = 0.2). (For interpretation of the references to color in this figure legend, the reader is referred to the web version of this article.)

3.2. Transmission-Bit-Rate Asymmetric Partitioning (TRaP)

Although PDPP3 with symmetric partitioning presents some resource usage advantages against DPP and PDPP2, performing such partitioning asymmetrically may offer further opportunities for network performance optimization. In TRsP approach, equal transmission rates are distributed among the link-disjoint multipaths regardless their physical characteristics or their spectral efficiencies (η [(b/s)/Hz]). Since each of such paths may have different physical lengths (meaning the allowance of modulation formats with different spectral efficiencies) and/or different hop counting, it might be interesting to allocate the service's transmission bit rate asymmetrically (TRaP) among the routes by assigning larger fractions of bit rates in paths that employ higher spectral efficiencies and/or hop counting; and vice versa.

Hence, under TRsP, the P link-disjoint routes $r_1, \ldots, r_p, \ldots, r_P$ assigned for a service receive the same amount of B_s (evaluated by Eq. (2)). On the other hand, under TRaP, each route r_p is assigned with a different value of transmission bit rate, referred to as $B_s^{\langle p \rangle}$. There are several different possible choices/combinations for the values of $B_s^{\langle p \rangle}$. To ensure the maximum allowed squeezing value (β) for any possible single-link failures (i.e. SLA compliance), the constraint in Eq. (5) must be satisfied.

$$\left(\sum_{p=1}^{P} B_s^{\langle p \rangle}\right) - B_s^{\langle q \rangle} \geq (1-\beta)\, B_r \quad \forall q \in \{1, \ldots, P\}\,. \tag{5}$$

Moreover, notice that by assuming TRaP, link-failures in distinct routes generate different squeezed amount in the transmission bit rate. Thus, we introduce in this paper the effective percentage of service's transmission bit rate reduction ($\beta_{eff}^{\langle p \rangle}$) during a single-link failure in route r_p. The value of $\beta_{eff}^{\langle p \rangle}$ can be evaluated by

$$\beta_{eff}^{\langle p \rangle} = \begin{cases} 0 & ,if \quad \sum_{\substack{q=1 \\ q \neq p}}^{P} B_s^{\langle q \rangle} \geq B_r \\ \dfrac{B_r - \sum_{\substack{q=1 \\ q \neq p}}^{P} B_s^{\langle q \rangle}}{B_r} & ,otherwise. \end{cases} \tag{6}$$

The summation in Eq. (6) stands for the total sum of the transmission bit rate that remains active when a single-link failure occurs in route r_p. Notice that, under TRaP, the evaluation of α for a service remains unaltered from the one shown in Eq. (4) except by the fact that now $B_t = B_s^{\langle 1 \rangle} + \cdots + B_s^{\langle P \rangle}$.

We illustrate in Fig. 2 a practical example of how TRaP can be efficient to improve the use of the available fiber bandwidth (frequency slots) , where we assume LD-MPR (P = 3), BSP (with β = 0.25) and the establishment of B_r = 200 Gb/s service between the nodes 0 and 6. The three selected routes r_1, r_2 and r_3 are shown in blue lines. In the example, we assume that routes r_1 and r_2 admit $\eta_1 = \eta_2 = 3$ (b/s)/Hz, whereas route r_3 admits only $\eta_3 = 1$ (b/s)/Hz, since it is longer than r_1 and r_2. Frequency slots are assumed as 12.5 GHz wide. Figs. 2(a) and 2(b) correspond, respectively, for the symmetric (TRsP) and a possible asymmetric (TRaP) partitioning.

In Fig. 2(a), the same amount of transmission bit rate (B_s = 75 Gb/s, evaluated using Eq. (2)) is allocated in routes r_1, r_2 and r_3, which means the occupation of 2 slots per link on routes r_1 and r_2 and 6 slots per link on route r_3 (by observing B_s and η for each route). Thus, the total number of used slots is $(2 \times 2) + (2 \times 2) + (4 \times 6) = 32$. On the other hand, on the asymmetric partitioning shown in Fig. 2(b), a greater amount of transmission bit rate ($B_s^{\langle 1 \rangle} = B_s^{\langle 2 \rangle} = 112.5$ Gb/s) is allocated on routes that are shorter and use more efficient modulation formats (r_1 and r_2), whereas a lower bit-rate portion ($B_s^{\langle 3 \rangle} = 37.5$ Gb/s) is allocated on r_3. In this case, the bandwidth usage is 3 slots per link for all routes. Therefore, the number of used slots is $(2\times3)+(2\times3)+(4\times3) = 24$. This simple example shows that assignments under TRaP can indeed reduce network slot usage when compared to TRsP. Notice that Eq. (5) still holds for $B_s^{\langle 1 \rangle}$, $B_s^{\langle 2 \rangle}$ and $B_s^{\langle 3 \rangle}$, and that there are several different combinations for choosing proper values for $B_s^{\langle 1 \rangle}$, $B_s^{\langle 2 \rangle}$ and $B_s^{\langle 3 \rangle}$ (that still satisfy Eq. (5)), each of one leading to different total bandwidth usage and effective squeezing ratio. It is not an easy task to choose an optimized suitable combination of asymmetrical traffic partitioning, since there are several source–destination node pairs, with routes with different characteristics and under distinct congestion in a dynamic-traffic scenario. We address this problem in Section 7.

As previously mentioned, in LD-MPR with TRaP, breaks in distinct links generate different transmission bit rate squeezing. For example, in Fig. 2(b) while a link-failure in either routes r_1 or r_2 generates a $\beta_{eff}^{\langle 1 \rangle} = \beta_{eff}^{\langle 2 \rangle} = 0.25$, a link failure in r_3 generates a $\beta_{eff}^{\langle 3 \rangle} = 0$. This characteristic can be strategically used to minimize the average transmission bit rate squeezing experienced by the allocated services during a link-failure event.

In order to estimate this characteristic, we introduce a new metric in this paper, which is the average transmission bit rate squeezing factor ($\bar{\beta}$) for each service allocated in the network. This parameter corresponds to the expected value of β_{eff} when a failure occurs in either of the routes assigned to a given service. This is evaluated by weighting the effective traffic squeezing related to a failure in a specific route and the probability of failure episode on that route, as shown in

$$\bar{\beta} = \frac{\sum_{p=1}^{P} \beta_{eff}^{\langle p \rangle} \times P(p)}{\sum_{p=1}^{P} P(p)}, \tag{7}$$

in which $P(p)$ is the probability of a failure occurring on route r_p given that a single-link failure has occurred. Considering the scenario in which all L network links have the same failure probability ($1/L$) and link failures occur independently, then $P(p)$ is

$$P(p) = 1 - \prod_{h=0}^{h_p - 1} \left(1 - \frac{1}{L-h}\right), \tag{8}$$

in which, h_p is the hop counting of route r_p.

We use again the scenario shown in Fig. 2 to assess, as an illustrative example, the impact of using either TRsP or TRaP strategies on $\bar{\beta}$. For instance, under TRsP regime, the service in Fig. 2(a) presents $\bar{\beta} = 0.25$, since a single-link failure in whatever service route results the same transmission bit rate (B_x = 150 Gb/s), as $\beta_{eff}^{\langle 1 \rangle} = \beta_{eff}^{\langle 2 \rangle} = \beta_{eff}^{\langle 3 \rangle} = 0.25$. Under TRaP regime, on the other hand, the service shown in Fig. 2(b) presents the following evaluation for $\bar{\beta}$:

$$\bar{\beta} = 2 \times 0.25 \times \left[1 - \left(1 - \frac{1}{8}\right)\left(1 - \frac{1}{7}\right)\right]$$

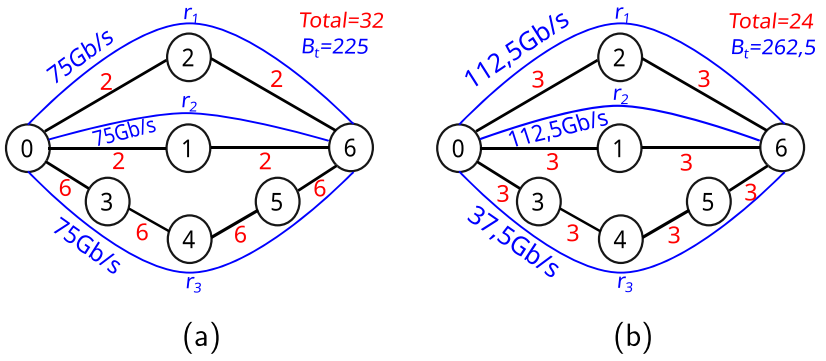

Fig. 2. Example of connection between nodes 0 and 6 (B_r = 200 Gb/s, β = 0.25 and slot bandwidth 12.5 GHz), established by: (a) symmetric partitioning and (b) asymmetric partitioning. (For interpretation of the references to color in this figure legend, the reader is referred to the web version of this article.)

$$+0\times\left[1-\left(1-\frac{1}{8}\right)\left(1-\frac{1}{7}\right)\left(1-\frac{1}{6}\right)\right]=0.125.$$

The value $L = 8$ is considered for the evaluation, since the network in the example has 8 links. Note that the value of the last term in the numerator is null, which is an outcome from the fact that a failure in r_3 does not impose transmission bit rate squeezing to the service, since the traffic of the two remaining paths (r_1 and r_2) add to 225 Gb/s, which is greater than B_r. Hence, the example shows that an efficient traffic partitioning, as proposed by TraP, may result in lower average traffic squeezing, which is beneficial for improving network operators' quality of service. This motivates the development of an efficient optimization technique for mitigating the expected value of bandwidth squeezing under single-link failures, as in Fig. 2(b).

The metrics $\bar{\beta}$ and α as presented so far are used to assess a single specific service. However, since each service z shows different values for both parameters, we now explicitly include this dependence by writing these parameters as $\bar{\beta}^{\langle z\rangle}$ and $\alpha^{\langle z\rangle}$. Then, it is possible to compute $\bar{\beta}_N$ and $\bar{\alpha}_N$ as the average of such metrics for all established services in the network as:

$$\bar{\beta}_N=\frac{\sum_{z=1}^{Z}\bar{\beta}^{\langle z\rangle}}{Z}\quad\text{and}\quad\bar{\alpha_N}=\frac{\sum_{z=1}^{Z}\alpha^{\langle z\rangle}}{Z},\tag{9}$$

in which Z is the number of established protected services.

4. Optimization problem formulation

In this section we describe the optimization problem considered in this paper. Let us start setting the symbols used in the formulation. The network is represented by the graph $\mathcal{T}(N, L)$, composed by $|N|$ vertices (network nodes) and $|L|$ edges (network links). All possible different types of network services are represented by the tuple $R(i, j, B_r, \beta)$, which represents the service's source node i ($i \in \{1,\ldots,|N|\}$), destination node j ($j \in \{1,\ldots,|N|\}$), its requested transmission bit rate B_r ($B_r \in \mathcal{B}_r = \{b_1,\ldots,b_{TR}\}$) (where $\mathcal{B}_r$ represents the set of allowed service's transmission bit rates, and TR its cardinality), and the maximum allowed traffic squeezing factor, β. There is an available ordered set of K pre-computed candidate groups of P link-disjoint paths between each source and destination node pairs $i-j$, defined as $\mathcal{G}^{\langle i,j\rangle} = \{g_1^{\langle i,j\rangle},\ldots,g_k^{\langle i,j\rangle},\ldots,g_K^{\langle i,j\rangle}\}$, in which $g_k^{\langle i,j\rangle}$ is composed by an ordered set of P link-disjoint routes in $\mathcal{T}(N, L)$, i.e. $g_k^{\langle i,j\rangle} = \{r_{1,k}^{\langle i,j\rangle},\ldots,r_{p,k}^{\langle i,j\rangle},\ldots,r_{P,k}^{\langle i,j\rangle}\}$, where $r_{p,k}^{\langle i,j\rangle}$ and $r_{q,k}^{\langle i,j\rangle}$ are link-disjoint routes for $p \neq q$, $\forall i, j, k$. The manner how the set $\mathcal{G}$ is both generated and used in the routing procedure is described in Section 6.

The optimization procedure finds how the transmission bit rate of each service $R(i, j, B_r, \beta)$ is asymmetrically divided among the P pre-computed routes. It means to find the values for $B_s^{\langle p,i,j,B_r\rangle}$ $\forall p, i, j, B_r$. Note that we have included the indexes i, j and B_r to the previously defined $B_s^{\langle p\rangle}$ to express the fact that the asymmetrical transmission bit rate partitioning considered here is dependent on both source and destination $i-j$ node pair and the requested transmission bit rate. Therefore, the optimization considered in this work may be defined as in Table 2.

5. Overview of algorithms and strategies proposed in this paper

Fig. 3 presents a flowchart that illustrates the interaction among the algorithms and strategies proposed in this article employed to build the proposed Optimized Partitioning Dedicated Path Protection (OPDPP) framework (described in Section 7). The optimization problem defined in Table 2/Section 4 is addressed using the multi-objective optimizer NSGA-II (red block in Fig. 3). Details on the optimization process setup are described in Section 7. The optimization block assumes $B_s^{\langle p,i,j,B_r\rangle}$ as design variables (green block in Fig. 3), while the optimization objectives (fitness functions shown in the purple block) are the network's average transmission bit rate squeezing factor ($\bar{\beta}_N$, calculated using Eq. (9)) and the network blocking probability (BP), obtained from an optical network simulator (gray block in Fig. 3 and described in Section 8). The network simulator generates a large number of services to be embedded in the network (assuming a dynamic/stochastic traffic pattern) which simulates the process of setting up and tearing down services in a real network. The optical network simulator evaluates the probability that a given service does not find available resources in the network to accommodate it at its arrival time, which is referred to as the network blocking probability and evaluated by

$$BP=\frac{\Gamma_{Service\_Blocked}}{\Gamma_{Service\_Blocked}+\Gamma_{Service\_Accepted}}.\tag{10}$$

Here, $\Gamma_{Service\_Blocked}$ and $\Gamma_{Service\_Accepted}$ represent the numbers of blocked and accepted services, respectively, during the simulation. The contributions/novelties proposed in this article concerning the implementation feasibility of the new FARgdp concept are detailed in Section 6 through Algorithms 1, 2, and 3, as well as depicted in Fig. 3 through the blocks representing the generation of candidate groups of link-disjoint routes (yellow block, Algorithm 3), FARgdp routing (cyan block, Algorithm 1), and the DPGR-multi-P algorithm (brown block, Algorithm 2).

6. Proposed fixed-alternate routing using groups of disjoint paths (FARgdp)

In classical fixed-alternate routing schemes, the route to be used to allocate each incoming service is selected from an ordered list of K pre-calculated routes. One tries to allocate the incoming service in the first route of that list, if there are no resources in this first route, the second route in the list is tried and so on.

In the scenario considered in this work (BSP, LD-MPR and TRaP), each incoming service is allocated using not only one route, but using a set of P disjoint routes. In this scenario, groups of candidate link-disjoint routes should be sequentially tried rather than a single route. To the best of our knowledge we are proposing in this paper a fixed-alternate routing algorithm that considers such set of candidate groups of link-disjoint paths.

Table 2
Definition of the optimization problem.

Given:	Physical topology $\mathcal{T}(N, L)$, the statistical modeling of the dynamic traffic, the traffic matrix, set of allowed transmission bit rates, B_r, K candidate groups of P link-disjoint paths between each source and destination node pairs $i-j$, $\mathcal{G}^{\langle i,j\rangle}$, and the squeezing factor, β, set in the SLA.
Find:	$B_s^{\langle p,i,j,B_r\rangle}$ $\forall p, i, j, B_r$
Subject to:	$\sum_{p=1,p\neq q}^{P} B_s^{\langle p,i,j,B_r\rangle} \geq (1-\beta)\, B_r \;\; \forall q \in \{1,\ldots,P\}$ (From Eq. (5)).
Minimize:	Simultaneously the overall network blocking probability (BP) and the network average transmission bit rate squeezing factor ($\bar{\beta}_N$). Achieving this necessitates employing a multi-objective optimization procedure.

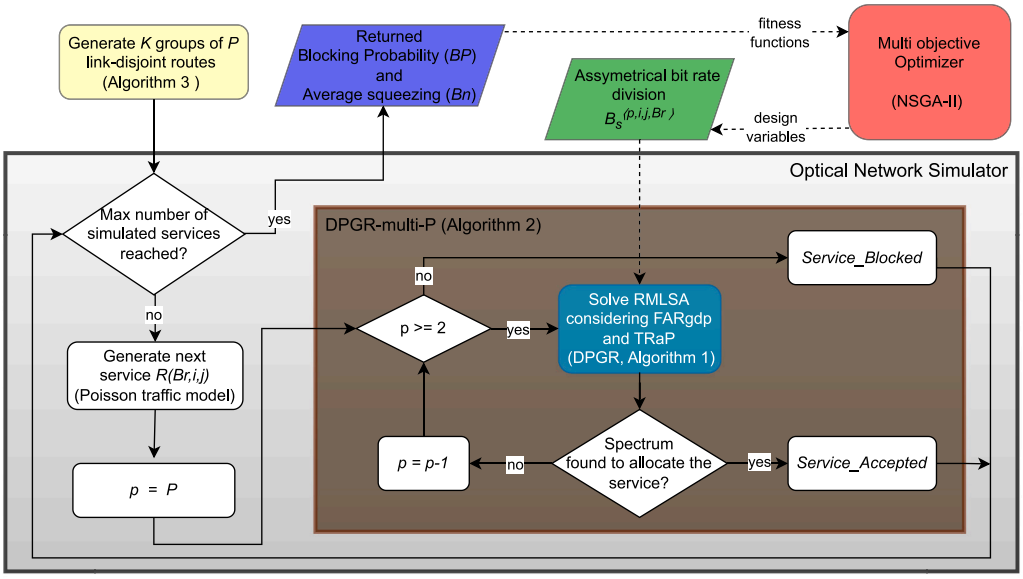

Fig. 3. Overview on the proposed Optimized Partitioning Dedicated Path Protection (OPDPP) framework. The figure shows a flowchart that illustrates the interaction among the algorithms and strategies proposed in this article. (For interpretation of the references to color in this figure legend, the reader is referred to the web version of this article.)

Let the incoming service $R(i, j, B_r, \beta)$ be divided into the following P independent transmission bit rate flows: $\mathcal{B} = \{B_s^{\langle 1,i,j,B_r\rangle}, B_s^{\langle 2,i,j,B_r\rangle}, \ldots, B_s^{\langle P,i,j,B_r\rangle}\}$. The candidate set of groups of link-disjoint paths $\mathcal{G}^{\langle i,j\rangle} = \{g_1^{\langle i,j\rangle}, \ldots, g_k^{\langle i,j\rangle}, \ldots, g_K^{\langle i,j\rangle}\}$ is then considered to allocate $R(i, j, B_r, \beta)$. Each candidate group $g_k^{\langle i,j\rangle} = \{r_{1,k}^{\langle i,j\rangle}, r_{2,k}^{\langle i,j\rangle}, \ldots, r_{P,k}^{\langle i,j\rangle}\}$ is composed by an ordered set of P disjoint routes in $\mathcal{T}(N, L)$. Upon a request $R(i, j, B_r, \beta)$ arrival, the algorithm tries to use the routes that belong to the first (i.e. $k = 1$) group $g_1^{\langle i,j\rangle}$ in $\mathcal{G}^{\langle i,j\rangle}$. It means that $B_s^{\langle 1,i,j,B_r\rangle}$ is assigned to route $r_{1,1}^{\langle i,j\rangle}$, $B_s^{\langle 2,i,j,B_r\rangle}$ is assigned to route $r_{2,1}^{\langle i,j\rangle}$ and so on. If $g_1^{\langle i,j\rangle}$ fails in the route assignment for $R(i, j, B_r, \beta)$, then the second ($k = 2$) group $g_2^{\langle i,j\rangle}$ in $\mathcal{G}^{\langle i,j\rangle}$ is tried and then $B_s^{\langle 1,i,j,B_r\rangle}$ is assigned to route $r_{1,2}^{\langle i,j\rangle}$, $B_s^{\langle 2,i,j,B_r\rangle}$ is assigned to route $r_{2,2}^{\langle i,j\rangle}$ and so on. Note that the described process consists on the routing procedure, and any spectrum assignment algorithm may be used to perform the spectral allocation.

The proposed fixed-alternate routing mechanism employing groups of link-disjoint paths (FARgdp) follows the above mentioned steps, and we named it as disjoint-path-group routing (DPGR). The details on DPGR procedure is presented in Algorithm 1. The function $SA(B_s^{\langle p,i,j,B_r\rangle}, r_{p,k}^{\langle i,j\rangle})$ is any spectrum assignment algorithm used to allocate the transmission bit rate $B_s^{\langle p,i,j,B_r\rangle}$ using the route $r_{p,k}^{\langle i,j\rangle}$. In this paper we assume that the spectrum assignment algorithm is aware of the available transmission modulation formats and its quality of transmission (QoT) requirements in order to determine both the required number of frequency slots and maximum transmission reach. By considering that the set $\mathcal{G}^{\langle i,j\rangle}$ is pre-computed and available, the dominant time-consuming part of Algorithm 1 is the $SA(B_s^{\langle p,i,j,B_r\rangle}, r_{p,k}^{\langle i,j\rangle})$ call, which means that the time complexity of the algorithm is $O(K \cdot P)$.

In the main proposal of this paper, we use as routing, modulation format and spectrum assignment algorithm (RMSA) [27] the procedure DPGR-multi-P, presented in Algorithm 2. It consists of making successive calls to DPGR, starting with $p = P$ and decrementing the value of p at each attempt until a solution is found. Note that the call for DPGR($\mathcal{B}, 1, K, i, j, B_r$), i.e. $P = 1$, is not considered because such case does not provide protection. The time complexity of DPGR-multi-P is $O(K \cdot P^2)$.

Another novelty presented in this article is the strategy used to generate the set $\mathcal{G}^{\langle i,j\rangle}$. In works found in the literature [6,18], some authors use the Bhandari's algorithm [40] to find the groups of P link-disjoint routes. The strategy consists on running Bhandari's algorithm to find a number Q ($Q > P$) of link-disjoint routes and then combine these Q routes to form groups of P link-disjoint routes. Clearly this strategy is not able to find all possible groups of P link-disjoint routes available in the topology, which limits the applicability of the FARgdp strategy. We address this problem in this paper by evaluating all possible groups of P link-disjoint routes between a given source and destination nodes $i-j$. The algorithm used to evaluate such groups is described in Algorithm 3. This algorithm returns the ordered set $\mathcal{G}^{\langle i,j\rangle}$ containing K groups of P link-disjoint routes. These groups are ordered in ascending order of total hop counting of its routes.

Line 1 of Algorithm 3 computes all routes between each source–destination node pair $(i-j)$ in $\mathcal{T}(N, L)$ using Depth-First Search (time complexity $O(N + L)$), where N is the number of nodes and L is the number of links in the topology. Line 2 forms all possible groups of P link-disjoint paths between $i-j$ (time complexity $O((A!)/[(A-P)! \cdot P!])$). Lines 3 and 4 compute the hop and distance sum for all found W

Algorithm 1 DPGR($\mathcal{B}, P, K, i, j, B_r$) pseudo-code

1: Acquire the set $\mathcal{G}^{\langle i,j\rangle}$ considering P and K;
2: $Success \longleftarrow false$;
3: $k, p \longleftarrow 1$;
4: **while** (($k \leq K$) **and not** ($Success$)) **do**
5: $Success \longleftarrow true$;
6: **while** (($p \leq P$) **and** ($Success$)) **do**
7: **if** ($SA(B_s^{\langle p,i,j,B_r\rangle}, r_{p,k}^{\langle i,j\rangle})$ succeed) **then**
8: Allocate $B_s^{\langle p,i,j,B_r\rangle}$ using the route $r_{p,k}^{\langle i,j\rangle}$ and the available modulation format with highest spectral efficiency that meets QoT requirements;
9: $p \longleftarrow p + 1$;
10: **else**
11: Dislocate all previously allocated routes;
12: $Success \longleftarrow false$;
13: $p \longleftarrow 1$;
14: **end if**
15: **end while**
16: $k \longleftarrow k + 1$;
17: **end while**
18: **if** ($Success$) **then**
19: **return** $Service\_Accepted$;
20: **else**
21: **return** $Service\_Blocked$;
22: **end if**

Algorithm 2 DPGR-multi-P($\mathcal{B}, P, K, i, j, B_r$) pseudo-code

1: **for** ($p = P$ **to** 2, $p--$) **do**
2: **if** (DPGR($\mathcal{B}, p, K, i, j, B_r$) = $Service\_Blocked$) **then**
3: Continue to next p;
4: **else**
5: **return** $Service\_Accepted$;
6: **end if**
7: **end for**
8: **return** $Service\_Blocked$;

Algorithm 3 GroupsGeneration($\mathcal{T}, P, K, i, j$)

Require: Topology= $\mathcal{T}(N, L)$; Number of groups K;
1: Find the set $\mathcal{A}^{\langle i,j\rangle}$ containing all possible loopless routes between $i-j$ pairs in $\mathcal{T}$;
2: Compute the set $\mathcal{W}_P^{\langle i,j\rangle} = \{w_1^{\langle i,j\rangle}, w_2^{\langle i,j\rangle}, \ldots, w_W^{\langle i,j\rangle}\}$ containing all W groups of P disjoint paths between the pair $i-j$ by testing all possible combinations of P routes in $\mathcal{A}^{\langle i,j\rangle}$;
3: Compute the hop sum h_x of all disjoint routes that compose the group $w_x^{\langle i,j\rangle}$
4: Compute the distance sum d_x of all disjoint routes that compose the group $w_x^{\langle i,j\rangle}$
5: Sort the groups $w_x^{\langle i,j\rangle}$ inside $\mathcal{W}_P^{\langle i,j\rangle}$ in ascending order of h_x (ties are broken by sorting in ascending order of d_x and any remaining ties are broken randomly);
6: $\mathcal{G}^{\langle i,j\rangle} \longleftarrow$ the first K groups in $\mathcal{W}_P^{\langle i,j\rangle}$;
7: Sort, in ascending order of hop count, the routes inside all groups $g_k^{\langle i,j\rangle} \in \mathcal{G}^{\langle i,j\rangle}$ (ties are broken sorting in ascending order of route length and any remaining ties are broken randomly);
8: **return** $\mathcal{G}^{\langle i,j\rangle}$;

groups of P routes (both lines show time complexity $O(W \cdot P)$). Line 5 sorts the groups in ascending order of total number of hops (time complexity $O(W^2)$). Line 6 selects the first K groups after the sorting (time complexity $O(K)$). Line 7 sorts the routes inside each group in ascending order of number of hops (time complexity $O(K \cdot P^2)$). Note that the worst time complexity is verified in line 2. However, this combinatorial time complexity is polynomial for small values of P (low number of transmission bit rate divisions), which is the case in our application. Moreover, Algorithm 3 may be executed in offline manner by making a look-up table in the groups of routes during the routing operation. Thus, by building such look-up table, the high time complexity required by Algorithm 3 does not impact the quick response required by the RMSA procedure on a dynamic-traffic network.

7. Proposed Optimized Partitioning Dedicated Path Protection (OPDPP) framework

The proposed optimized protection framework aims to carry out a careful partitioning of services' required transmission bit rate among the group of link-disjoint routes for each source–destination node pairs in order to simultaneously reduce the BP and $\bar{\beta}_N$ as defined in Table 2. We named the proposed framework as Optimized Partitioning Dedicated Path Protection (OPDPP). The implementation of the proposed OPDPP takes place in two phases: the optimization phase, henceforth named as offline-phase, and an operational phase, henceforth named as online-phase:

- Offline-phase — The optimization problem shown in Table 2 is solved in the offline-phase. Algorithm 2 and non-optimized values of $B_s^{\langle p,i,j,B_r\rangle}$ are used to solve RMSA problem for each incoming service request, as shown in Fig. 3. The selected optimization algorithm (in our case the NSGA-II) makes several attempts for different values of $B_s^{\langle p,i,j,B_r\rangle}$ in order to identify their optimized values. This optimization is performed in a multi-objective way with the goal of reducing, simultaneously, the network performance figures of merit shown in "Minimize" line of Table 2. In order to find values for these figures of merit, the optical network simulator is employed (see Sections 5 and 8). Note that, if the optimization algorithm takes a long time to perform its task, it will not impact the time required to solve the RMSA algorithm during the day-to-day operations of the network. This phase takes place before the real time network operation when its control plane needs to quickly solve RMSA for each network service request arrival.
- Online-phase — After the offline phase, the most suitable (optimized) values for $B_s^{\langle p,i,j,B_r\rangle}$ are already found. Algorithm 2 is integrated into the network control plane but using single and fixed (optimized) values for the parameters $B_s^{\langle p,i,j,B_r\rangle}$. The online phase works as shown in Fig. 3, but without the multi-objective optimizer block.

The details on how the optimization procedure is performed in the offline-phase is discussed in Section 7.1, whereas the online-phase only uses Algorithm 2 for RMSA solutions. For the sake of clarity and simplicity, we shall refer to the near optimum protection RMSA algorithm, derived from the application of the OPDPP framework, as OPDPP algorithm throughout this study.

7.1. Proposed optimizer to perform asymmetrical partitioning

In order to solve the multi objective optimization problem defined in Table 2, we have used the Non-dominated Sorting Genetic Algorithm (NSGA-II) optimization procedure [41]. NSGA-II is known to be suitable to find near optimum solutions for various different optimization problems [27,42–45]. Several other optimization metaheuristics could be utilized instead, but it is out of the scope of this paper to find the best metaheuristic to solve the problem defined in Table 2.

NSGA-II is a type of a genetic algorithm which iteratively evolves a set of individuals towards the simultaneous optimization of the multiple objective functions. In the instance of the NSGA-II used in the paper, each individual represents a possible choice for $\mathcal{B}$ =

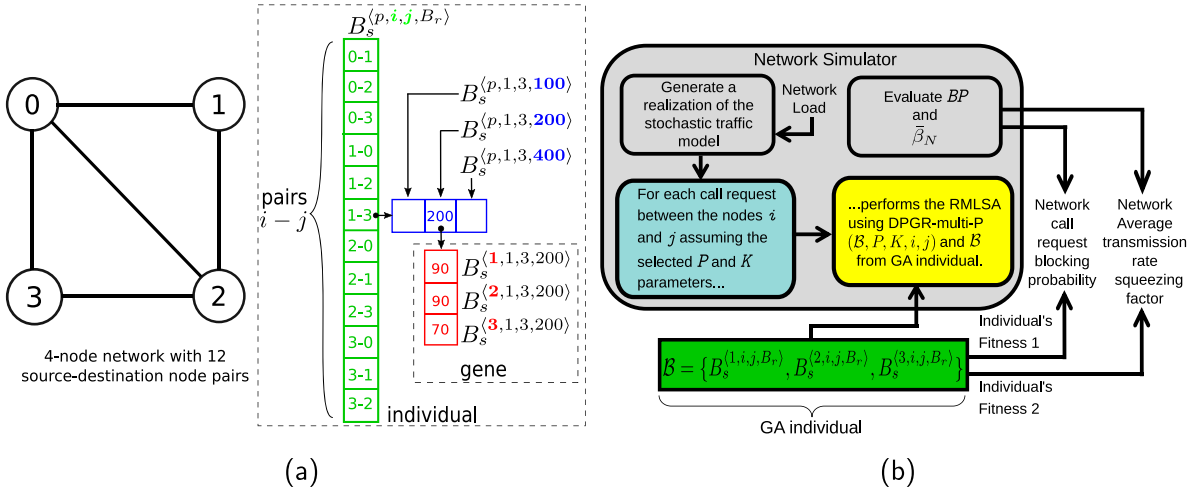

Fig. 4. (a) Example of the individual structure for the scenario of a 4-node network considering three link-disjoint routes ($P = 3$) and three service transmission rates ($TR = 3$). (b) Block diagram that represents how the fitness of each individual is evaluated. (For interpretation of the references to color in this figure legend, the reader is referred to the web version of this article.)

$\{B_s^{\langle 1,i,j,B_r\rangle}, B_s^{\langle 2,i,j,B_r\rangle}, \ldots, B_s^{\langle P,i,j,B_r\rangle}\}$. Fig. 4(a) shows an example of the individual representation for the case of a 4-node network considering the availability of three link-disjoint routes ($P = 3$) and three service's transmission bit rates ($TR = 3$). Each individual is represented by a three-dimensional tensor. The first dimension stands for the entries corresponding to each source–destination pair (in green), the second stands for the entries corresponding to service's transmission bit rates (in blue) and the third stands for the entries corresponding to the values of partial transmission bit rate designated for each link-disjoint path (in red). We select this last vector as the individual's gene. Thus, each gene actually stores a valid asymmetric division, among P link-disjoint routes, of the transmission bit rate required by a service request (B_r) that yet comply with the set β in a one link failure scenario. The discrete set of possibilities for each gene and the generation of such set is discussed in Section 7.2.

Note that each individual represents a possible solution for the problem and how well an individual solves the optimization problem is determined by valuing its fitness functions. In Fig. 4(b) we show how each individual information (in our approach) is used to obtain its fitness functions values. The green filled rectangle comprises the previously discussed transmission bit rates partitions $\mathcal{B} = \{B_s^{\langle 1,i,j,B_r\rangle}, B_s^{\langle 2,i,j,B_r\rangle}, \ldots, B_s^{\langle P,i,j,B_r\rangle}\}$ "stored" by each individual. The two fitness functions of each individual are evaluated using a network simulator (shown in gray box) that simulates a large set of service requests under dynamic traffic regime (shown in light blue box). The RMSA algorithm (which is a building block of the network simulator itself and is depicted in yellow box) is solved for each simulated incoming service by using the $\mathcal{B}$ information from the individual alongside with Algorithm 2. Then, after the generation of several service requests, the simulator returns both the resultant overall network blocking probability (BP) and the average network squeezing factor ($\bar{\beta}_N$) (evaluated using Eq. (9)) to be assigned as the individual's fitness.

The iterative process of the NSGA-II optimizer used in this work is the same used in [2] with the modifications in the initialization, crossover and mutation operators. The population is composed by Q individuals and they are initialized at random. Each gene of each individual is randomly selected (uniform distribution) among the available choices (see Section 7.2).

Two individuals I_1 and I_2 are selected for crossover operation using the roulette wheel approach [46]. In each mating operation, we apply the uniform crossover [47] between parents I_1 and I_2 to generate new offspring individuals I_3 and I_4. The parent's genes are swapped, with probability of p_c, to generate offspring I_3 and I_4. In each iteration of the algorithm, $Q/2$ crossover operations are executed to generate Q new individuals. This population created by multiple crossover operations are also subjected to the mutation operation. Each gene of each individual of this population is mutated with the probability of p_m. Each mutated gene is filled with a randomly (uniform distribution) new content, selected among the available possibilities (see Section 7.2).

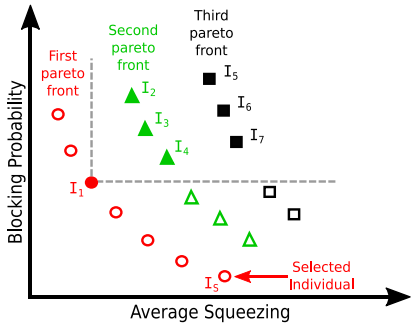

Fig. 5. Example of Pareto fronts and dominance criteria in a multi-objective optimization process.

At the end of the iterations, the NSGA-II returns sets of non dominated solutions named as Pareto fronts. Three Pareto fronts are exemplified in Fig. 5. In this figure, the individuals found by NSGA-II are plotted accordingly their BP and $\bar{\beta}_N$. The individual I_1 presents lower value in at least one fitness function and non-higher value in the other fitness function than the individuals I_2 to I_7. Thus, by definition, I_1 is said to "dominates" I_2 to I_7 (meaning that the solution I_1 shows a better trade-off on the considered fitness functions than I_2 to I_7). If one aims to minimize simultaneously the BP and $\bar{\beta}_N$, it is clear from the plot that individuals that achieve the best trade-off between BP and $\bar{\beta}_N$ belongs to the first Pareto front. In this work, we use the individual with lowest BP value (I_s in the plot) as the optimized solution obtained at the end of the offline-phase. Note that, since the optimization is done in a multi-objective way, this chosen solution represents not only the one that provides the lowest BP, but also the one that provides the lowest $\bar{\beta}_N$ available for such low value of BP.

7.2. Considered combinations of transmission bit rate partitioning

Each gene from a NSGA-II individual stores a valid combination that asymmetrically distributes the B_r for a given service request $R(i, j, B_r, \beta)$ among P link-disjoint routes and yet obeying the restriction imposed

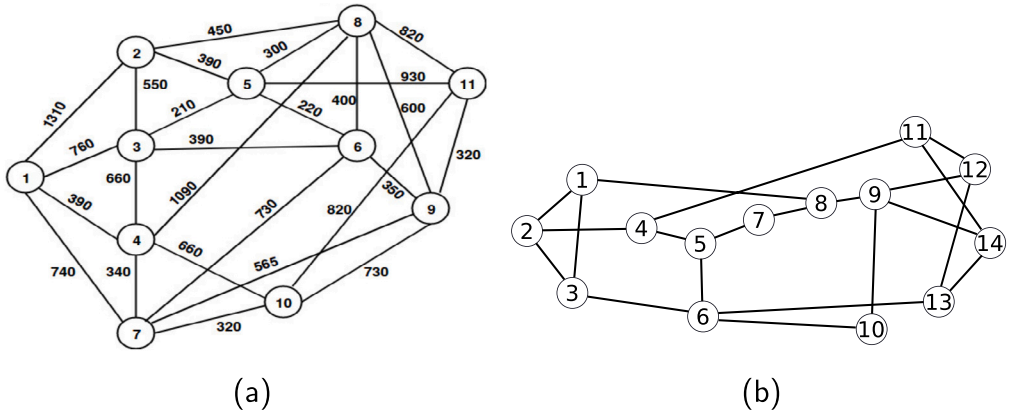

Fig. 6. Topologies: (a) COST239 and (b) NSFNET.

by the SLA on β. Clearly, there are several possibilities for such combinations. Let $C^{\langle P,\beta,\alpha,B_r\rangle} = \{c_1, c_2, \ldots, c_C\}$ represent all such combinations, whereas c_x is composed by a set of P bitrates $c_x = \{B^{\langle 1\rangle}, B^{\langle 2\rangle}, \ldots, B^{\langle P\rangle}\}$. In order to reduce the number of combinations available for each gene (and consequently speeding up the NSGA-II convergence) we apply the following constraints on $B^{\langle p\rangle}$ and β.

$$\begin{aligned} \beta &\le 1/P \\ B^{\langle 1\rangle} = B^{\langle 2\rangle} &= B_r(1-\beta) \text{ if } P = 2 \\ \gamma_i B_r \le B^{\langle p\rangle} &\le \gamma_f B_r \text{ if } P > 2 \\ B^{\langle p\rangle} &\in \{\gamma_i B_r, \gamma_i B_r + \gamma_s, \gamma_i B_r + 2\gamma_s, \ldots \gamma_f B_r\} \text{ if } P > 2 \end{aligned} \tag{11}$$

in which γ_i and γ_f sets, respectively, holds the lower and the higher values allowed for $B^{\langle p\rangle}$, whereas γ_s sets its discretization step. By applying such restrictions, one obtains the reduced set $\tilde{C}^{\langle P,\beta,\alpha,B_r\rangle} = \{\tilde{c}_1, \tilde{c}_2, \ldots, \tilde{c}_{\tilde{C}}\}$ such that $\tilde{C}^{\langle P,\beta,\alpha,B_r\rangle} \subset C^{\langle P,\beta,\alpha,B_r\rangle}$. In this paper we consider as valid gene combinations the ones in $\tilde{C}^{\langle P,\beta,\alpha,B_r\rangle}$ set, built using $\gamma_i = 0.2$, $\gamma_f = 0.8$, and $\gamma_s = 0.05$ Gb/s.

8. Simulation setup

An elastic optical network simulator, extended from [48], is used to carry out simulations results. The simulator is able to evaluate the network blocking probability under dynamic traffic conditions. The service requests arrive randomly following a Poisson process with holding time exponentially distributed. Call requests are established through an unidirectional circuit-switched lightpath. The results were obtained for two network physical topologies (shown in Fig. 6): COST239 (Fig. 6(a)), composed by 11 nodes, 24 bidirectional links and average node degree of 4.72 , and NSFNET (Fig. 6(b)), composed by 14 nodes, 21 bidirectional links and average node degree of approximately 3. The mutation probability used in NSGA-II (p_m) is set to provide about 2 gene mutations (on average) per individual, which leads to $P_m = 0.006$ for COST239 topology and $P_m = 0.0037$ for NSFNET topology. Moreover, we used 100 generations, 50 individuals and a crossover probability $p_c = 0.5$. We evaluate the noise accumulation in optical layer according to the model described in [27]. The amplified spontaneous emission (ASE) noise generated by the EDFA amplifiers is considered as physical impairment for OSNR evaluation. EDFA noise figure of 5 dB is assumed. Each link is composed by several spans (80 km of SSMF fiber plus an EDFA that compensates for the fiber loss). SSMF attenuation coefficient of 0.2 dB/km is used. To reduce the time required for simulations, we opted to assume 128 frequency slots per link. However, the strategies proposed in this study operate independently of the number of slots assumed per link. The accumulated noise is evaluated for each call request. The required OSNR of each modulation format depends on transmission bit rate and the desired BER after forward error correction (FEC) [26,49]. We have assumed the maximum acceptable BER equals to 10^{-3}, which is a common value for hard-decision FECs. The minimal optical signal-to-noise ratio ($osnr_{Th}$) for each modulation format (in linear units) [50] is

$$osrn_{Th} = \frac{R_b \cdot snr_b}{2 \cdot B_{Ref}}, \tag{12}$$

in which snr_b is the signal-to-noise ratio per bit, B_{Ref} is the reference bandwidth ($B_{Ref} = 12.5$ GHz) and R_b, in bits per second (b/s), is the overall bit rate (in both polarizations). The assumed simulation parameters of optical transponders are: traffic demand options $\mathcal{B}_r \in \{100, 200, 400\}$ Gb/s, launch power of 0 dBm, input signal OSNR of 30 dB and QAM-$\{4, 8, 16, 32, 64\}$ and BPSK modulation formats. The offered loads employed in each simulation scenario are selected in order to keep the call request blocking probability achieved by the proposed OPDPP approximately between 10^{-5} and 10^{-2}.

We compare the results obtained by the proposed OPDPP against 5 other algorithms detailed in Table 3. In this study, our hypothesis is that the implementation of FARgdp and TRaP strategies can potentially reduce the network blocking probability. To validate this hypothesis, we chose to use, as benchmark, simple algorithms (DPP and PDPP) that do not employ both strategies and compare them against our proposals that employ FARgdp and TRaP. Through this comparison, we can analyze the impact on the blocking probability solely due to the application of the proposed strategies. The algorithm PDPP3S is the same proposed by Assis et al. [12]. Notice that PDPP3S may also serve as a benchmarking purpose. The routing mechanism assumed by PDPP3S involves the selection of the shortest disjoint routes in terms of hops. We implement this functionality here by giving to PDPP3S the first group of routes found by algorithm 3. It corresponds to set $K = 1$. This routing strategy mirrors the functionality of Bhandari's algorithm [40], which similarly identifies the shortest disjoint routes based on a specified metric (minimum number of hops in our case). Consequently, in terms of route discovery, the routes identified by Bhandari's algorithm correspond to those found by PDPP3S. The algorithms $DPPS_F$, $PDPP2S_F$ and $PDPP3S_F$ are proposed in this paper and they are enhanced (by the consideration of FARgdp approach) versions of their counterparts proposed in [12]. $PDPP3S_{FM}$ is also proposed in this paper and it is an enhancement of PDPP3S that uses both the FARgdp approach and DPGR-multi-P() algorithm. As shown in Table 3, all 5 algorithms may be implemented as especial cases of either DPGR() (Algorithm 1) or DPGR-multi-P() (Algorithm 2). Particularly, note that PDPP3S can be implemented as an especial case of the proposed DPGR() algorithm by assuming TRsP, $K = 1$ (*i.e.* no application of FARgdp strategy), $P = 3$ for the node pairs that have 3 link-disjoint routes and $P = 2$ otherwise. All simulated algorithms use, as the spectrum assignment process ($SA(B_s^{\langle p,i,j,B_r\rangle}, r_{p,k}^{\langle i,j\rangle})$), the first-fit policy [25].

Table 3
Parameters and descriptions of protection algorithms investigated in this paper.

Algorithm	RMSA	Apply FARgdp?	P	K	Partitions $\mathcal{B}$	Proposed in
$DPPS_F$	DPGR()	Yes	2	10	$B_s^{\langle 1,i,j,B_r\rangle} = B_r$ and $B_s^{\langle 2,i,j,B_r\rangle} = (1-\beta)B_r \ \forall\ i,j$.	This paper[a]
$PDPP2S_F$	DPGR()	Yes	2	10	$B_s^{\langle p,i,j,B_r\rangle} = B_s \ \forall\ p,i,j,\ B_s$ from Eq. (2).	This paper[a]
PDPP3S	DPGR()	No	3/2	1	$P=3$ if there is 3 link-disjoint routes between nodes i,j and $P=2$ otherwise. $B_s^{\langle p,i,j,B_r\rangle} = B_s \ \forall\ p,\ B_s$ from Eq. (2).	[12]
$PDPP3S_F$	DPGR()	Yes	3/2	10	Same of the previous line.	This paper[a]
$PDPP3S_{FM}$	DPGR-multi-P()	Yes	3	10	$B_s^{\langle p,i,j,B_r\rangle} = B_s \ \forall\ p,\ B_s$ from Eq. (2).	This paper[a]
OPDPP	DPGR-multi-P()	Yes	3	10	$B_s^{\langle p,i,j,B_r\rangle}$ optimized and different for each pair $i-j$	this paper

[a] The algorithms are enhanced versions of their counterparts found in [12] but proposed in this paper.

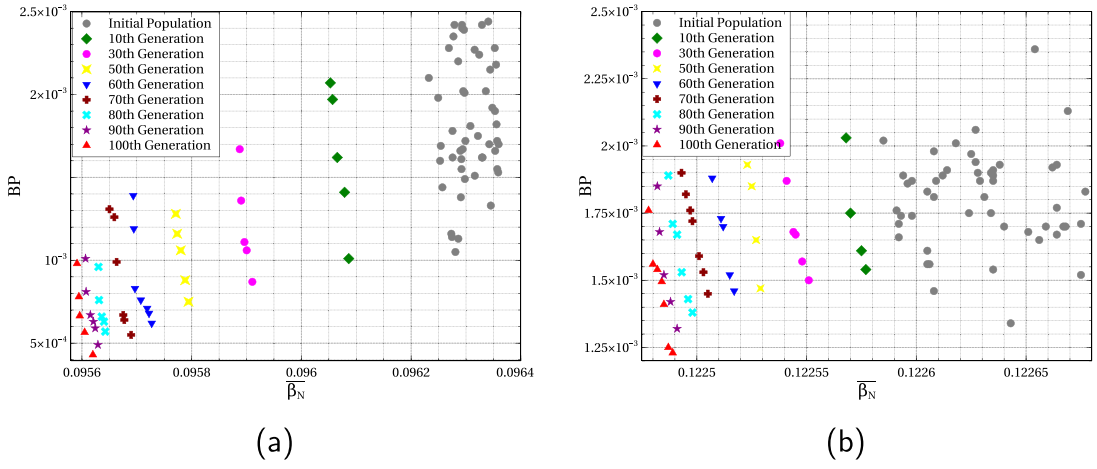

Fig. 7. Convergence of NSGA-II algorithm for (a) COST239 (250 erlang) and (b) NSFNET (50 erlang). Solutions found are plotted in a call request blocking probability versus network average transmission bit rate squeezing factor graph. The initial population and first Pareto fronts per generations are shown using the labeled colors and symbols. (For interpretation of the references to color in this figure legend, the reader is referred to the web version of this article.)

9. Simulation results

9.1. Convergence analysis (offline-phase)

In our approach, the first step to solve the optimization problem defined in Section 4 is the application of NSGA-II optimizer in offline-phase (as mentioned in Section 7.1). NSGA-II is an iterative algorithm and we can analyze the convergence of the algorithm along its iterative process (named as generations) as shown in Fig. 7. The result for COST239 at an offered network load of 250 erlangs is shown in Fig. 7(a) and for NSFNET at 50 erlangs in Fig. 7(b). Fig. 7 relates the call request blocking probability with the network average transmission bit rate squeezing factor for some solutions found by the NSGA-II during its optimization process: initial population (gray symbols) and first Pareto front at the end of a given generation. The symbols with the same shape/color belong to first Pareto front found by NSGA-II after the labeled number of generations.

Note that the solutions in the first Pareto front of a given generation dominate the solutions in the first Pareto front of the previous generations, which shows the convergent trend of the algorithm. Furthermore, low improvement can be observed between generations 90 and 100 in both topologies. Therefore, the solution with the lowest BP value after 100 generations is fixed to be used by OPDDP during the online-phase (the results shown in next subsections).

9.2. Blocking probability analysis (online-phase)

Fig. 8 shows the plots for service request blocking probability (BP) as a function of the offered network load for all investigated protection algorithms described in Table 3 in COST239 topology. The simulations are carried out assuming either $\beta = 0.2$ (Figs. 8(a) and 8(b)) or $\beta = 0.3$ (Fig. 8(c)) and either no guard band (Figs. 8(a) and 8(c)) or one slot of guard band (Fig. 8(b)). The blocking probabilities shown are the mean value for 10 independent simulations. We have also evaluated, for each simulated point, the associated error bars for a 95% confidence interval. We have decided to suppress those error bars from the graphs because they are too narrow and difficult to visualize in the graphs. Similar analysis for NFSNET topology is shown in Fig. 9.

Figs. 8 and 9 show that the proposed OPDDP outperforms all investigated protection schemes regardless the topology, β and considered number of guard band slots. Moreover, OPDDP far outperforms the original PDPP3S (shown in pink/x symbols curves in the graphs) strategy proposed in [13]. It also can be noted from the plots that the relative differences between the BPs found by OPDDP and $PDPP3S_{FM}$ (second best algorithm in all graphs) are more pronounced in COST239 than in NSFNET topology. Possibly this outcome is due to the fact that the COST239 network is a more connected topology (high average node degree) than NSFNET, which results in a greater diversity in the number of available disjoint routes and, consequently, more optimization opportunities to be explored by both OPDDP and multi path strategy.

Figs. 8 and 9 can also be used to quantify the improvements in BP achieved by both strategies: fixed-alternate groups of link-disjoint routes (FARgdp) and successive attempts in number of link-disjoint routes considered (Multi-P). In all simulated scenarios, it is possible to note that the BP found by the PDPP3S is significantly reduced when the FARgdp strategy is adopted, i.e. by using the $PDPP3S_F$ algorithm. Moreover, further BP reduction is verified when FARgdp and Multi-P strategies are simultaneously adopted, although the reduction is large in COST239 and almost negligible in NSFNET (compare the BP achieved by algorithms $PDPP3S_F$ and $PDPP3S_{FM}$ in each graph).

As discussed in Section 1, one of the main disadvantages of using multipath routing is the possible necessity of adding guard band slots to each considered path. The impact on BP of considering GB slots as guard band can be analyzed, in our simulations, by comparing the results achieved by $PDPP2S_F$ and $PDPP3S_F$ in Figs. 8(a) and 8(b) (for COST239 topology) and in Figs. 9(a) and 9(b) (for NSFNET topology).

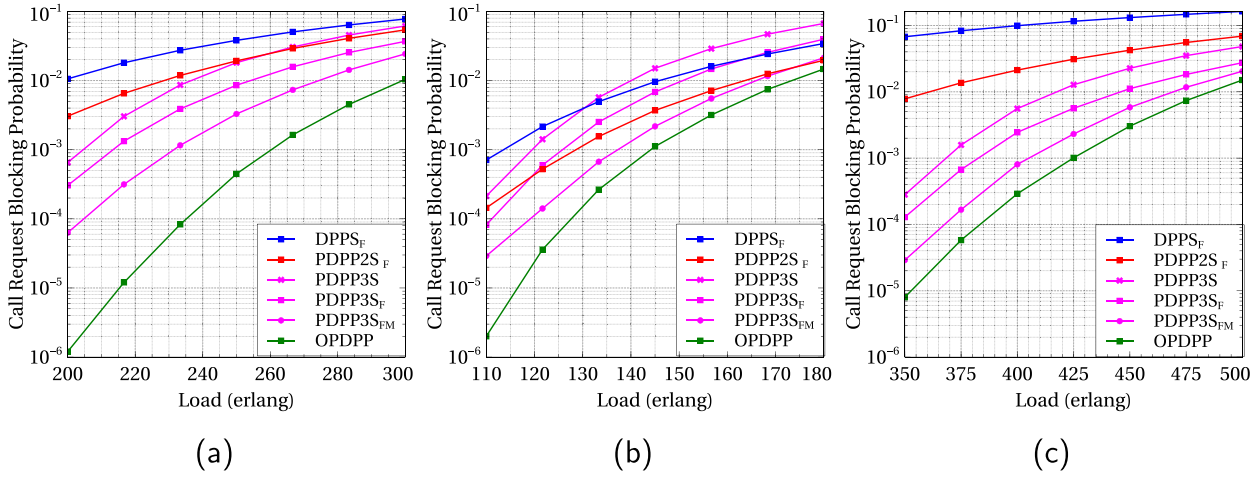

Fig. 8. COST239 call request blocking probability per offered network load for: (a) $\beta = 0.2$ and $GB = 0$; (b) $\beta = 0.2$ and $GB = 1$ and (c) $\beta = 0.3$ and $GB = 0$. (For interpretation of the references to color in this figure legend, the reader is referred to the web version of this article.)

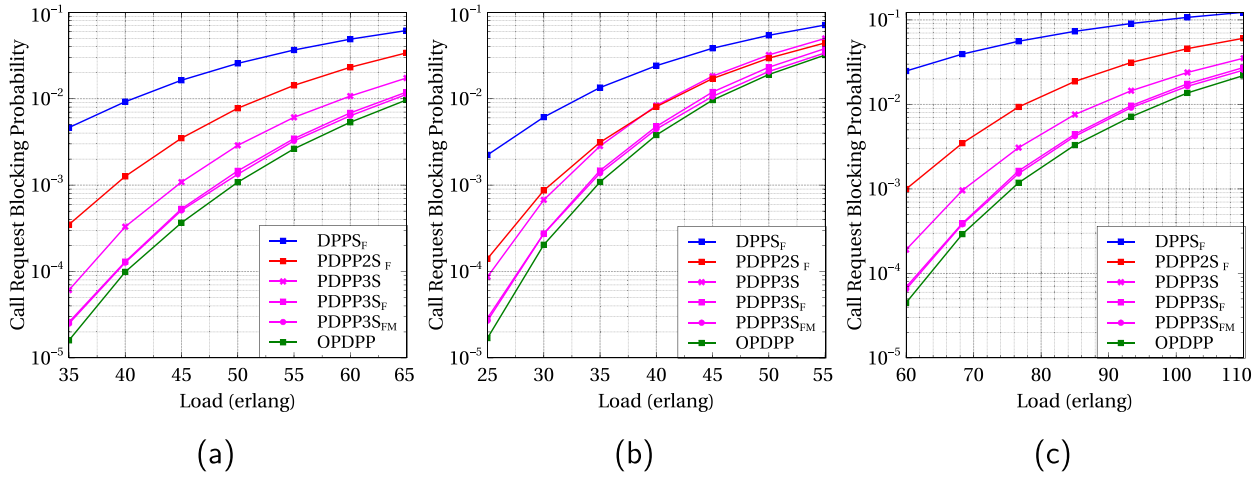

Fig. 9. NSFNET call request blocking probability per load for: (a) $\beta = 0.2$ and $GB = 0$; (b) $\beta = 0.2$ and $GB = 1$ and (c) $\beta = 0.3$ and $GB = 0$. (For interpretation of the references to color in this figure legend, the reader is referred to the web version of this article.)

For $GB = 0$ (Figs. 8(a) and 9(a)), PDPP3S$_F$ far outperforms PDPP2S$_F$ in both topologies. Similarly, for $GB = 1$ (Figs. 8(b) and 9(b)) PDPP3S$_F$ still outperforms PDPP2S$_F$ in NSFNET topology. Nevertheless, the opposite is verified in COST239 topology for offered loads higher than 120 erlangs. Although PDPP3S$_F$ enables spectrum resource saving in comparison to PDPP2S$_F$, it requires higher number of guard band slots. Thus, BP curves obtained for PDPP3S$_F$ and PDPP2S$_F$ get closer for $GB = 1$ when compared to $GB = 0$ scenario.

This can be noted in the NSFNET, but the effect is more evident in the COST239 topology in which even a performance inversion between the algorithms is perceived. A possible explanation for such inversion is: since COST239 has higher average node degree than NSFNET, more connections are allocated with three than with two paths, which requires a larger number of guard band slots. One can note that at about 120 erlangs it is verified an inversion in the BP curves found by PDPP3S$_F$ and PDPP2S$_F$ in COST239 topology.

Finally, as expected, for a certain level of BP, the network operation assuming $\beta = 0.3$ and $GB = 0$ supports more load than the network operation under $\beta = 0.2$ and $GB = 0$ which supports more load than the network operation under $\beta = 0.2$ and $GB = 1$. Using as example OPDPP in COST239 topology and the BP level of 10^{-3}, the network supports approximately: 425 erlangs for $\beta = 0.3$ and $GB = 0$ (Fig. 8(c)), 260 erlangs for $\beta = 0.2$ and $GB = 0$ (Fig. 8(a)) and 145 erlangs for $\beta = 0.2$ and $GB = 1$ (Fig. 8(b)).

9.3. Other network performance analysis (online-phase)

Table 4 shows the results for $\bar{\beta_N}$, $\bar{\alpha_N}$ and the average network resource utilization υ_N in all simulated scenarios obtained for the algorithms PDPP3S, PDPP3S$_{FM}$ and OPDPP in COST239 (250 erlang) and NSFNET (50 erlang) topologies. The table also shows the percentage of source–destination pairs designated to use either symmetric (TRsP) or asymmetric (TRaP) strategy (lines "Symmet. %" and "Asymmet. %"). Remember that in the case of the proposed OPDPP this designation is done during the offline phase. We compute υ_N as the ratio between the summation of used slots by all the accepted calls multiplied by its respective holding time and total network slots available multiplied by the simulation time.

In all simulated scenarios and topologies, the OPDPP algorithm finds lower values for BP, $\bar{\beta_N}$ and υ_N as compared against either PDPP3S$_{FM}$ or PDPP3S. There are two exceptions for this statement (marked in bold in the table) in NSFNET topology in which PDPP3S achieves lower (by a very low margin) υ_N values if compared against OPDPP. It means that the OPDPP provides a solution that, at the same time, presents less blocking events, lower (or almost even) average spectral occupancy of the network, and lower average reduction of transmission bit rate in the occurrence of single link failures. On the other hand, in all investigated cases, OPDPP needs to allocate higher amount of total transmission bit rate (i.e. higher $\bar{\alpha_N}$) in comparison against to either PDPP3S$_{FM}$ or PDPP3S.

Table 4
Results overview for COST239 (250 erlangs) and NSFNET (50 erlangs) topologies.

COST239		$\beta = 0.2$ $GB = 0$ 250 erlangs			$\beta = 0.2$ GB=1 145 erlangs			$\beta = 0.3$ GB=0 425 erlangs	
	PDPP3S	PDPP3S$_{FM}$	OPDPP	PDPP3S	PDPP3S$_{FM}$	OPDPP	PDPP3S	PDPP3S$_{FM}$	OPDPP
PB	0.018157	0.00329	0.000447	0.01506	0.002176	0.001113	0.012776	0.002311	0.001011
$\bar{\beta_N}$	0.2	0.2	0.092084	0.2	0.2	0.097271	0.3	0.3	0.13657
$\bar{\alpha_N}$	0.2	0.202617	0.352868	0.2	0.202269	0.349325	0.05	0.051418	0.108953
υ_N	0.462457	0.474066	0.447148	0.40548	0.412686	0.39805	0.528305	0.538407	0.527921
Symmet.%	100	100	1.1	100	100	3.03	100	100	8.2
Asymmet.%	0	0	98.9	0	0	96.97	0	0	91.8
NSFNET		$\beta = 0.2$ $GB = 0$ 50 erlangs			$\beta = 0.2$ GB=1 40 erlangs			$\beta = 0.3$ GB=0 85 erlangs	
	PDPP3S	PDPP3S$_{FM}$	OPDPP	PDPP3S	PDPP3S$_{FM}$	OPDPP	PDPP3S	PDPP3S$_{FM}$	OPDPP
PB	0.002887	0.001336	0.001081	0.008337	0.004448	0.003797	0.007605	0.004206	0.003306
$\bar{\beta_N}$	0.2	0.2	0.119673	0.2	0.2	0.12069	0.3	0.3	0.172654
$\bar{\alpha_N}$	0.309359	0.30973	0.420479	0.308341	0.309113	0.419017	0.144676	0.145355	0.271179
υ_N	0.233944	0.235014	0.232793	**0.252776**	0.255146	0.253846	**0.298958**	0.302418	0.301811
Symmet.%	100	100	1.93	100	100	2.48	100	100	5.31
Asymmet.%	0	0	98.07	0	0	97.52	0	0	94.69

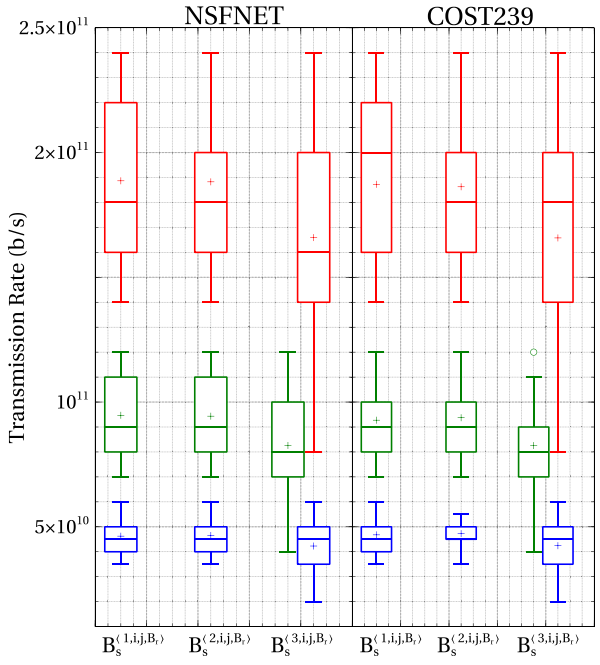

Fig. 10. Transmission bit rate distribution among the partitions ($B_s^{\langle 1,i,j,B_r\rangle}$, $B_s^{\langle 2,i,j,B_r\rangle}$ and $B_s^{\langle 3,i,j,B_r\rangle}$) for each traffic demand option (100 Gb/s blue boxes, 200 Gb/s green boxes and 400 Gb/s red boxes), defined by GA solution, for $\beta = 0.2$ and $GB = 0$, plotted as a box chart for NSFNET (50 erlangs) and COST239 (250 Elangs). (For interpretation of the references to color in this figure legend, the reader is referred to the web version of this article.)

It can also be seen from the table that the optimized solution found by OPDPP (for COST239, $\beta = 0.2$ and $GB = 0$) have designated the asymmetrical distribution of transmission bit rate between the three routes for 98.9% of source–destination node pairs, whereas the symmetrical distribution is adopted for only 1.1% of the pairs. Moreover, notice that a similar outcome is verified in the other simulated scenarios, i.e. the OPDPP solution have designated the asymmetrical distribution for more than 90% of the source–destination node pairs in all simulated cases.

We have investigated not only the percentage of source–destination node pairs that are using either symmetrical of asymmetrical strategy, but also the statistics regarding the amount of transmission bit rate that is designated by OPDPP (NSGA-II optimization) to each of the three partitions of each source–destination node pairs. The analysis for the two topologies are shown in box-and-whisker plot in Fig. 10. The vertical axis stands for the transmission bit rate designated to each of the three partitions that are labeled in the horizontal axis. Each box is drawn from first to third quartile, the horizontal line and the symbol drawn inside the box denote, respectively, the median and the mean, the whiskers are drawn based on 1.5 times the interquartile range rule and circles are the outliers data points. The red, green and blue boxes stand, respectively, for the 400 Gb/s, 200 Gb/s and 100 Gb/s services. Notice that there is a trend on the OPDPP choice to allocate higher amount of transmission bit rate in the first two partitions than in the third partition. It makes sense because the routes serving the partitions are sorted in decreasing order of spectral efficiency, with highest spectral efficiency available route being allocated to serve the first partition and so on.

10. Conclusion

In this paper we propose a novel protection scheme for elastic optical networks under dynamic traffic named as OPDPP. It considers the multipath routing scenario in which the services' transmission bit rate are asymmetrically divided among multiple link-disjoint paths, as well as, they may be squeezed (reduced) when the services are affected by a single-link failure. The OPDPP uses a multi-objective genetic algorithm that defines, for each pair of network's nodes, how the services transmission bit rate should be partitioned among the link-disjoint paths. The aim of the optimization procedure is to minimize, simultaneously, the network blocking probability and the average squeezed transmission bit rate experienced by the services under a single-link failure. A metric to quantify the average squeezed transmission bit rate in the network is also proposed and introduced in the paper. We carried out several simulations to assess the OPDPP performance. In all investigated scenarios (COST239/NSFNET topologies, maximum allowed squeezing factor β of 0.2 and 0.3 and paths with and without guard bands), the OPDPP was able to find lower values of blocking probabilities when compared with other 5 algorithms (one algorithm is from the literature, whereas the other four are enhanced versions of previously proposed algorithms). Moreover, we also propose in this paper the new concept of fixed-alternate routing using groups of link-disjoint paths (FARgdp). In FARgdp concept, the classical fixed-alternate routing that considers a set of candidate routes is transformed into a set of groups of candidate routes, each group containing P link-disjoint routes. We apply the FARgdp concept to

propose two protection algorithms (DPGR and DPGR-Multi-P), as well as, we apply it to enhance four algorithms found in the literature. In all investigated scenarios, the algorithms that apply the FARgdp concept achieved lower values of blocking probabilities (by a large margin) when compared against their counterpart algorithms that do not apply it.

CRediT authorship contribution statement

Henrique A. Dinarte: Writing – review & editing, Writing – original draft, Software, Resources, Investigation. **Karcius D.R. Assis:** Visualization, Validation, Methodology. **Daniel A.R. Chaves:** Writing – review & editing, Writing – original draft, Visualization, Validation, Supervision, Project administration, Methodology, Investigation, Formal analysis, Conceptualization. **Raul C. Almeida Jr.:** Visualization, Validation, Supervision, Project administration, Methodology, Investigation, Formal analysis, Conceptualization. **Raouf Boutaba:** Writing – review & editing, Visualization, Validation, Supervision.

Declaration of competing interest

The authors declare the following financial interests/personal relationships which may be considered as potential competing interests: Daniel A. R. Chaves, Raul C. Almeida Jr., Karcius D. R. Assis reports financial support was provided by National Council for Scientific and Technological Development (CNPq). If there are other authors, they declare that they have no known competing financial interests or personal relationships that could have appeared to influence the work reported in this paper.

Data availability

No data was used for the research described in the article.

Acknowledgments

The auhtors thanks to Federal University of Pernambuco, Federal University of Bahia, University of Pernambuco, University of Waterloo, FACEPE, CAPES and CNPq.

References

[1] B.C. Chatterjee, N. Sarma, E. Oki, Routing and spectrum allocation in elastic optical networks: A tutorial, IEEE Commun. Surv. Tutor. 17 (3) (2015) 1776–1800, http://dx.doi.org/10.1109/COMST.2015.2431731.

[2] M. Cavalcante, H. Pereira, D. Chaves, R. Almeida, Optimizing the cost function of power series routing algorithm for transparent elastic optical networks, Opt. Switch. Netw. 29 (2018) 57–64, http://dx.doi.org/10.1016/j.osn.2018.05.001.

[3] K. Assis, R. Almeida, M. Reed, A. Santos, H. Dinarte, D. Chaves, H. Li, S. Yan, R. Nejabati, D. Simeonidou, Protection by diversity in elastic optical networks subject to single link failure, Opt. Fiber Technol., Mater. Devices Syst. 75 (2023) 103208, http://dx.doi.org/10.1016/j.yofte.2022.103208.

[4] C.J. Lira, R.C. Almeida, D.A. Chaves, Spectrum allocation using multiparameter optimization in elastic optical networks, Comput. Netw. 220 (2023) 109478, http://dx.doi.org/10.1016/j.comnet.2022.109478.

[5] C. Liu, K. Wang, W. Zhan, Y. Wang, B. Xiao, W. Gao, Multi-path routing spectrum allocation algorithm based on fragment sensing and energy saving, in: 2021 5th International Conference on High Performance Compilation, Computing and Communications, ACM, 2021, pp. 50–54, http://dx.doi.org/10.1145/3471274.3471283.

[6] S. Paira, J. Halder, U. Bhattacharya, M. Chatterjee, A novel fragmentation-aware and energy-efficient multipath routing and spectrum allocation for prioritized traffic in protected EONs, in: 2020 11th International Conference on Computing, Communication and Networking Technologies, ICCCNT, IEEE, 2020.

[7] P.M. Moura, N.L.S. da Fonseca, Multipath routing in elastic optical networks with space-division multiplexing, IEEE Commun. Mag. 59 (10) (2021) 64–69, http://dx.doi.org/10.1109/MCOM.111.2100331.

[8] H.M. Oliveira, N.L. da Fonseca, Multipath routing, spectrum and core allocation in protected SDM elastic optical networks, in: 2019 IEEE Global Communications Conference (GLOBECOM), IEEE, 2019, pp. 1–6.

[9] L. Ruiz, R.J. Durán Barroso, I. De Miguel, N. Merayo, J.C. Aguado, E.J. Abril, Routing, modulation and spectrum assignment algorithm using multi-path routing and best-fit, IEEE Access 9 (2021) 111633–111650, http://dx.doi.org/10.1109/ACCESS.2021.3101998.

[10] U. Ujjwal, N. Mahala, J. Thangaraj, Dynamic adaptive spectrum allocation in flexible grid optical network with multi-path routing, IET Commun. 15 (2) (2021) 211–223, http://dx.doi.org/10.1049/cmu2.12046, arXiv:https://ietresearch.onlinelibrary.wiley.com/doi/pdf/10.1049/cmu2.12046.

[11] K. Takeda, T. Sato, R. Shinkuma, E. Oki, Multipath provisioning scheme for fault tolerance to minimize required spectrum resources in elastic optical networks, Comput. Netw. 188 (2021) 107895.

[12] K.D. Assis, R.C. Almeida, H. Waldman, MILP formulation for squeezed protection in spectrum-sliced elastic optical path networks, in: 2012 International Symposium on Performance Evaluation of Computer & Telecommunication Systems, SPECTS, IEEE, 2012.

[13] K. Assis, S. Peng, R. Almeida, H. Waldman, A. Hammad, A. Santos, D. Simeonidou, Network virtualization over elastic optical networks with different protection schemes, J. Opt. Commun. Netw. 8 (4) (2016) 272–281.

[14] G. Junyent, J. Comellas, Using dual-path allocation for partial traffic protection in Elastic Optical Networks, in: 2017 19th International Conference on Transparent Optical Networks, ICTON, 2017, pp. 1–4, http://dx.doi.org/10.1109/ICTON.2017.8024849.

[15] A. Bhandari, J. Malhotra, A review on network survivability in optical networks, Int. J. Eng. Res. Appl. 5 (12) (2015) 97–101.

[16] J. Halder, T. Acharya, M. Chatterjee, U. Bhattacharya, On spectrum and energy efficient survivable multipath routing in off-line Elastic Optical Network, Comput. Commun. 160 (2020) 375–387, Publisher: Elsevier.

[17] J. Halder, T. Acharya, M. Chatterjee, u. Bhattacharya, E-s-RSM-RSA: A novel energy and spectrum efficient regenerator aware multipath based survivable RSA in offline EON, IEEE Trans. Green Commun. Netw. 5 (3) (2021) 1451–1466, http://dx.doi.org/10.1109/TGCN.2021.3075616.

[18] S. Paira, J. Halder, M. Chatterjee, U. Bhattacharya, On energy efficient survivable multipath based approaches in space division multiplexing elastic optical network: Crosstalk-aware and fragmentation-aware, IEEE Access 8 (2020) 47344–47356, Publisher: IEEE.

[19] R.C. Freitas, E.C.O. Santos, D.A.R. Chaves, H.A. Pereira, C.J.A. Bastos-Filho, J.F. Martins-Filho, A path protection algorithm based on OSNR for all-optical networks with wavelength sharing limitation, in: 2012 14th International Conference on Transparent Optical Networks, ICTON, 2012, pp. 1–4, http://dx.doi.org/10.1109/ICTON.2012.6253740.

[20] N. Shahriar, S. Taeb, S.R. Chowdhury, M. Zulfiqar, M. Tornatore, R. Boutaba, J. Mitra, M. Hemmati, Reliable slicing of 5G transport networks with bandwidth squeezing and multi-path provisioning, IEEE Trans. Netw. Serv. Manag. 17 (3) (2020) 1418–1431.

[21] K. Takeda, T. Sato, R. Shinkuma, E. Oki, Fault-tolerant multipath provisioning in elastic optical networks, in: 2019 24th OptoElectronics and Communications Conference (OECC) and 2019 International Conference on Photonics in Switching and Computing, PSC, 2019, pp. 1–3, http://dx.doi.org/10.23919/PS.2019.8818038.

[22] J. Halder, T. Acharya, U. Bhattacharya, On crosstalk aware energy and spectrum efficient survivable RSCA scheme in offline SDM-EON, J. Netw. Syst. Manage. 30 (1) (2022) 1–35.

[23] A.L.F. Lourenço, A.C. César, A deep neural network with a fuzzy multi-objective optimization model for fault analysis in an elastic optical network, Opt. Switch. Netw. 43 (2022) 100644.

[24] D.A.R. Chaves, D.O. Aguiar, C.J.A. Bastos-Filho, J.F. Martins-Filho, A methodology to design the link cost functions for impairment aware routing algorithms in optical networks, Photon. Netw. Commun. 22 (2) (2011/10/01) 133–150, http://dx.doi.org/10.1007/s11107-011-0314-2.

[25] R.C. Almeida, R.A. Delgado, C.J.A. Bastos-Filho, D.A.R. Chaves, H.A. Pereira, J.F. Martins-Filho, An evolutionary spectrum assignment algorithm for Elastic Optical Networks, in: 2013 15th International Conference on Transparent Optical Networks, ICTON, 2013, pp. 1–3, http://dx.doi.org/10.1109/ICTON.2013.6602858.

[26] M. Cavalcante, H. Pereira, D. Chaves, R. Almeida, Applying power series routing algorithm in transparent elastic optical networks, in: SBMO/IEEE MTT-S International Microwave and Optoelectronics Conference, 2015, pp. 1–5.

[27] M.A. Cavalcante, H.A. Pereira, D.A. Chaves, R.C. Almeida, Evolutionary multi-objective strategy for regenerator placement in elastic optical networks, IEEE Trans. Commun. 66 (8) (2018) 3583–3596.

[28] J.F. Martins-Filho, D.A.R. Chaves, C.J.A. Bastos-Filho, D.O. Aguiar, Intelligent and fast IRWA algorithm based on power series and particle swarm optimization, in: 2008 10th Anniversary International Conference on Transparent Optical Networks, Vol. 3, 2008, pp. 158–161, http://dx.doi.org/10.1109/ICTON.2008.4598679.

[29] D. Moniz, J. Pedro, N. Horta, J. Pires, Multi-objective framework for cost-effective OTN switch placement using NSGA-II with embedded domain knowledge, Appl. Soft Comput. 83 (2019) 105608, http://dx.doi.org/10.1016/j.asoc.2019.105608.

[30] S. Bouamama, C. Blum, J.-G. Fages, An algorithm based on ant colony optimization for the minimum connected dominating set problem, Appl. Soft Comput. 80 (2019) 672–686, http://dx.doi.org/10.1016/j.asoc.2019.04.028.

[31] X. Li, C. Yue, Y. Aneja, S. Chen, Y. Cui, An iterated Tabu search metaheuristic for the regenerator location problem, Appl. Soft Comput. 70 (2018) 182–194, http://dx.doi.org/10.1016/j.asoc.2018.05.019.

[32] Á. Rubio-Largo, M.A. Vega-Rodríguez, D.L. González-Álvarez, An improved multiobjective approach inspired by the flashing behaviour of fireflies for Traffic Grooming in optical WDM networks, Appl. Soft Comput. 21 (2014) 617–636, http://dx.doi.org/10.1016/j.asoc.2014.03.046.

[33] U. Bhanja, S. Mahapatra, A metaheuristic approach for optical network optimization problems, Appl. Soft Comput. 13 (2) (2013) 981–997, http://dx.doi.org/10.1016/j.asoc.2012.09.011.

[34] D.A.R. Chaves, C.J.A. Bastos-Filho, J.F. Martins-Filho, Multiobjective physical topology design of all-optical networks considering QoS and capex, in: National Fiber Optic Engineers Conference, Optica Publishing Group, 2010, JThA45, http://dx.doi.org/10.1364/NFOEC.2010.JThA45.

[35] M. Przewoźniczek, R. Goścień, K. Walkowiak, M. Klinkowski, Towards solving practical problems of large solution space using a novel pattern searching hybrid evolutionary algorithm – An elastic optical network optimization case study, Expert Syst. Appl. 42 (21) (2015) 7781–7796, http://dx.doi.org/10.1016/j.eswa.2015.05.040, URL https://www.sciencedirect.com/science/article/pii/S0957417415003760.

[36] I. Olszewski, Modified dual-path allocation algorithm in elastic optical networks, J. Netw. Syst. Manage. 28 (4) (2020) 1036–1054, http://dx.doi.org/10.1007/s10922-020-09513-4.

[37] L. Ruan, Y. Zheng, Dynamic survivable multipath routing and spectrum allocation in OFDM-based flexible optical networks, J. Opt. Commun. Netw. 6 (1) (2014) 77–85.

[38] R. Goścień, K. Walkowiak, M. Tornatore, Survivable multipath routing of anycast and unicast traffic in elastic optical networks, J. Opt. Commun. Netw. 8 (6) (2016) 343–355.

[39] D.S. Yadav, A. Chakraborty, B. Manoj, A multi-backup path protection scheme for survivability in elastic optical networks, Opt. Fiber Technol., Mater. Devices Syst. 30 (2016) 167–175.

[40] R. Bhandari, Survivable networks: algorithms for diverse routing, Springer Science & Business Media, 1999.

[41] K. Deb, A. Pratap, S. Agarwal, T. Meyarivan, A fast and elitist multiobjective genetic algorithm: NSGA-II, IEEE Trans. Evol. Comput. 6 (2) (2002) 182–197.

[42] B.V. Correia, R.C. Almeida, D.A. Chaves, H.A. Pereira, Optical inverse multiplexing technique applied to elastic optical networks, in: 2019 21st International Conference on Transparent Optical Networks, ICTON, IEEE, 2019.

[43] D.P. Pinto Roa, R. Lugo, Sub-graph based multicast protection in WDM networks: A multi/many-objective evolutionary algorithms approaches, in: XXIV Congreso Argentino de Ciencias de la Computación (La Plata, 2018), 2018.

[44] A. Eira, J. Santos, J. Pedro, J. Pires, Multi-objective design of survivable flexible-grid DWDM networks, J. Opt. Commun. Netw. 6 (3) (2014) 326–339.

[45] S. Verma, M. Pant, V. Snasel, A comprehensive review on NSGA-II for multi-objective combinatorial optimization problems, IEEE Access 9 (2021) 57757–57791.

[46] P. Lechowicz, K. Walkowiak, Genetic algorithm for routing and spectrum allocation in elastic optical networks, in: 2016 Third European Network Intelligence Conference, ENIC, IEEE, 2016, pp. 273–280.

[47] H.A. Dinarte, B.V. Correia, D.A. Chaves, R.C. Almeida Jr., Routing and spectrum assignment: A metaheuristic for hybrid ordering selection in elastic optical networks, Comput. Netw. 197 (2021) 108287.

[48] M.A. Cavalcante, H.A. Pereira, R.C. Almeida, SimEON: an open-source elastic optical network simulator for academic and industrial purposes, Photon. Netw. Commun. 34 (2) (2017) 193–201.

[49] D.A.R. Chaves, M.A. Cavalcante, H.A. Pereira, R.C. Almeida, A case study of regenerator placement and regenerator assignment in dynamic translucent elastic optical networks, in: 2016 18th International Conference on Transparent Optical Networks, ICTON, 2016, pp. 1–4, http://dx.doi.org/10.1109/ICTON.2016.7550658.

[50] R.-J. Essiambre, G. Kramer, P.J. Winzer, G.J. Foschini, B. Goebel, Capacity limits of optical fiber networks, J. Lightwave Technol. 28 (4) (2010) 662–701.

Henrique A. Dinarte has B.Sc. degree in Telecommunications Engineering, M.Sc. degree in Systems Engineering from University of Pernambuco and Ph.D degree in Electrical Engineering at Federal University of Pernambuco. He is a Adjunct Professor of Telecommunications Engineering at University of Pernambuco and research member of the Network Protocols Research Group (GPPR). His research activities focus on network protocol optimization, optical networks, network survivability,evolutionarycomputationinnetworksoptimizationand telecommunication projects.

Karcius Day R. Assis received the B.Sc. degree in electrical engineering from the Federal University of Paraíba, the M.Sc. degree from the Federal University of Espírito Santo, and the Ph.D. degree in electrical engineering from the University of Campinas. In 2010, he joined the Department of Electrical and Computer Engineering, Federal University of Bahia, Brazil, where he is an Associate Professor. He has currently returned to the High Performance Networks Group, Smart Internet Lab with the University of Bristol, U.K., as a Visiting Researcher. His research interests include optical networking, traffic engineering, resource management, network survivability, machine learning, future Internet, and telecommunication networks optimization and projects.

Daniel A.R. Chaves was born in Recife, Brazil. He received the B.Sc. (2006), M.Sc. (2008) and Ph.D. (2012) degrees in Electrical Engineering from Federal University of Pernambuco. He is Associate Professor of Computer Engineering at University of Pernambuco. Dr. Chaves is co-author of about 100 scientific papers related to optical networking, impairment aware RWA algorithms, network resilience, designing of all-optical and translucent networks and applications of computational intelligence in network optimization. He is IEEE Senior Member, associated researcher of Brazilian National Council for Scientific and Technological Development — CNPq and He is currently an associate editor for IEEE Access Journal. Google Scholar: https://scholar.google.com/citations? user=fM6l2AMAAAAJ&hl=en, ResearcherID: F-7915-2011.

Raul C. Almeida Jr. has B.Sc. in Electronics Engineering from the Federal University of Pernambuco (1999) and M.Sc. (2001) and Ph.D.(2004) in Electrical Engineering from UNICAMP. Between 2006 and 2011 he has joined the University of Essex, UK, as a Senior Research Officer and in 2012 he joined the Photonics Group, Department of Electronics and Systems of UFPE, in Recife — Brazil, where is currently an Associate Professor. Raul C. Almeida Jr. has experience in Electrical Engineering, focusing on Telecommunication Systems, and his main interests are in optical networks, traffic engineering, analytical modeling, evolutionary computation, future Internet and telecommunication networks optimization and projects.

Raouf Boutaba received his M.Sc. and Ph.D. degrees in computer science from Sorbonne University in 1990 and 1994, respectively. He is currently a University Chair Professor and the director of the School of Computer Science at the University of Waterloo. He is the founding Editor-in-Chief of IEEE Transactions on Network and Service Management (2007–2010) and served as the Editor-in-Chief of the IEEE Journal on Selected Areas in Communications (2018–2021). He is a Fellow of the IEEE, the Engineering Institute of Canada, the Canadian Academy of Engineering, and the Royal Society of Canada.